Supporting evidence for reverse cochlear traveling waves

W. Dong[a] and E. S. Olson
Department of Otolaryngology, Head and Neck Surgery, Columbia University, P & S 11-452, 630 West 168th Street, New York, New York 10032, USA

(Received 6 September 2007; revised 25 October 2007; accepted 27 October 2007; corrected 5 March 2007)

As a result of the cochlea's nonlinear mechanics, stimulation by two tones results in the generation of distortion products (DPs) at frequencies flanking the primary tones. DPs are measurable in the ear canal as oto-acoustic emissions, and are used to noninvasively explore cochlear mechanics and diagnose hearing loss. Theories of DP emissions generally include both forward and reverse cochlear traveling waves. However, a recent experiment failed to detect the reverse-traveling wave and concluded that the dominant emission path was directly through the fluid as a compression pressure [Ren, 2004, Nat. Neurosc. **7**, 333–334]. To explore this further, we measured intracochlear DPs simultaneously with emissions over a wide frequency range, both close to and remote from the basilar membrane. Our results support the existence of the reverse-traveling wave: (1) They show spatial variation in DPs that is at odds with a compression pressure. (2) Although they confirm a forward-traveling character of intraocochlear DPs in a broad frequency region of the best frequency, this behavior does not refute the existence of reverse-traveling waves. (3) Finally, the results show that, in cases in which it can be expected, the DP emission is delayed relative to the DP in a way that supports reverse-traveling-wave theory. © *2008 Acoustical Society of America.*
[DOI: 10.1121/1.2816566]

PACS number(s): 43.64.Kc, 43.64.Jb, 43.64.Bt [BLM] Pages: 222–240

I. INTRODUCTION

The discovery of oto-acoustic emissions was exciting because emissions are generated within the cochlea and detected within the ear canal (EC), thus providing a noninvasive view into cochlear mechanics (Kemp, 1978). However, the mechanism by which the emissions are transported out through the cochlea is not certain. The usual view was that a reverse-traveling wave was the dominant pressure mode, but recent results were interpreted as favoring a compression mode (Ren, 2004; He *et al.*, 2007). The present paper presents a comprehensive investigation, from cochlear mechanics to emissions, bearing on this question. The introduction below provides a background to cochlear pressure modes and reviews aspects of emission theory that are useful for the interpretation of our results.

Sound at the eardrum is transmitted via the middle ear to the auditory inner ear, the cochlea. Within the cochlea, the sound is carried along the cochlea's sensory tissue (organ of Corti) by a wave, known as the cochlear traveling wave (von Bekesy, 1960). The wave is supported by sensory tissue flexibility and fluid inertia and travels much slower than sound travels in water. It peaks at frequency-specific locations: low frequencies in the apex, high frequencies in the base. By measuring the mechanical response at one longitudinal location [Fig. 1(A)] and varying the frequency, the location's peak or "best" frequency (BF) is identified [Fig. 1(B)]. In a healthy cochlea at frequencies close to the BF the amplitude of the cochlear traveling wave is enhanced by active outer hair cell forces, which show saturating nonlinearity [Fig. 1(B)] (Robles and Ruggero, 2001; Cooper, 2003). The signature of the wave is found in the phase of the response to tonal stimuli, which can be delayed by several cycles relative to the input in the ear canal [Fig. 1(C)]. The phase versus frequency slope is termed the "group delay." In the intracochlear response, the group delay is large at frequencies close to the BF, reflecting the slow speed of the wave there. In passive cochlear models the slowing of the wave is related to its peaking, via conservation of energy (Lighthill, 1981). Species differences in the size of the group delay have been correlated with sharpness of frequency tuning (Shera *et al.*, 2002; Shera and Guinan, 2003; Ruggero and Temchin, 2007). Thus, the group delay is an interesting auditory metric.

In addition to launching the cochlear traveling wave along the sensory tissue, the vibration of the stapes compresses the cochlear fluid, causing a compression (sound-wave) pressure that exists along with the traveling-wave pressure. The compression pressure increases linearly with the intensity of stapes motion. The compression pressure mode was predicted theoretically by Peterson and Bogert (1950). It fills the cochlea approximately instantaneously (travels at the speed of sound in water) and can be roughly thought of as a background pressure that varies in time with the plunging motion of the stapes. (At high frequencies, standing-wave resonances are expected for this mode. Although interesting in its own right, this aspect of the compression pressure is not important for the present analysis.) The compression pressure is often called the cochlear "fast wave," as opposed to the slow cochlear traveling wave. The experimentally measured spatial variation of intracochlear pressure supports the idea that the pressure is composed of

[a]Electronic mail: wd2015@columbia.edu

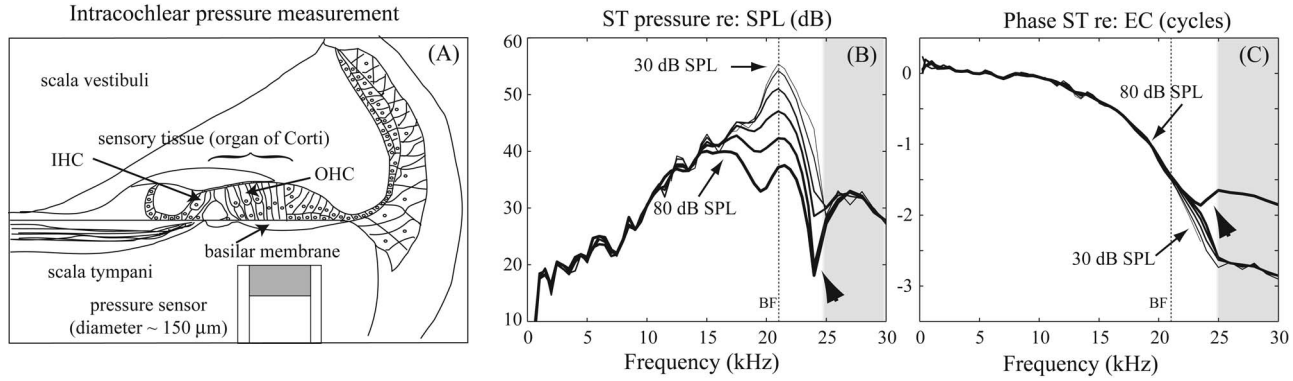

FIG. 1. Illustration of intracochlear pressure measurements and single tone response characteristics close to the BM. (A) Intracochlear pressure was measured in scala tympani (ST), close to or far from the sensory tissue's BM in the basal turn of the gerbil cochlea. The pressure sensor is shown to scale. Also indicated are the cochlear inner and outer hair cells, the mechanotransducers of audition. (B) and (C) Single-tone ST pressure responses measured close to the BM in turn one of the gerbil cochlea (wg81, 20 μm from BM, BF=21 kHz). (B) Amplitude normalized by the stimulus level in the EC. (C) Phase relative to the pressure in the EC. Significant aspects of cochlear mechanics are: (1) Cochlear nonlinearity: the normalized response curves fan out in the frequency region of the peak (15–25 kHz). 30 dB SPL responses showed a sharp peak at the BF of 21 kHz (dotted line), the 80 dB responses showed broader tuning with the peak shifted toward lower frequency. (2) Traveling wave: the phase of the response accumulated three complete cycles of delay relative to the stimulus in the ear canal. The phase changed most rapidly at frequencies around the BF. (3) Compression wave: at frequencies above 24 kHz, the phase changed little with frequency, which indicates that the fast wave dominated the responses. The amplitude in this frequency region was well above the noise floor and scaled linearly with SPL (gray band). (4) Interference between traveling and compression waves: the deep notch at 24 kHz with stimuli of 70 and 80 dB SPL corresponds to a region in which the phase jumps with level (arrowheads).

the sum of a traveling-wave mode and a compression mode (Olson, 1998, 1999, 2001, Dong and Olson, 2005b). Close to the BM and at frequencies near the local BF, rapid spatial pressure variations are present, evincing the fluid accelerations of the cochlear traveling wave. Such pressure variations were predicted in the 1970s by traveling-wave models (Steele and Taber, 1979a). At frequencies well above BF (where BM motion is very small), or far from the BM, the pressure is still large but is nearly spatially invariant, reflecting the lack of fluid acceleration and the dominance of the compression mode in this frequency region. (This behavior is shown, for example, in Fig. 4 of Dong and Olson (2005b); Fig. 10 of Olson (1998); Fig. 2 of Olson (1999); and Figs. 7 and 9 of Olson (2001)). In Figs. 1(B) and 1(C) of the present paper, the compression pressure region is identified by its linearity and relatively flat phase response (gray band). The destructive summation of the compression and traveling-wave modes produces notches in the pressure [arrowheads in Figs. 1(B) and 1(C)]. Because it can be mathematically uncoupled from the traveling-wave pressure and is not expected to lead to hair cell excitation (due to the very small motions it gives rise to), the compression pressure has been neglected in most cochlear models.

The cochlea's nonlinear mechanics produce distortion. For example, when two pure tones are used as stimulus, the response of a healthy cochlea contains a family of tones at frequencies corresponding to algebraic combinations of the input frequencies, termed "distortion products" (DPs). After being generated, a DP might travel apically to its own BF place, as demonstrated in both perceptual studies and intracochlear measurements (Goldstein, 1967; Robles *et al.*, 1997). The DPs also emerge from the cochlea, travel through the middle ear, and are detected in the EC as a DP otoacoustic emission (DPOAE) (Kemp, 1978). DPOAEs exhibit characteristic behavior: the amplitude contains frequency- and level-dependent notches ("fine structure") and the DPOAE phase versus frequency can be either nearly flat or rapidly varying as the frequency of the primaries is swept at a constant ratio.

Based on these and other observations, the analysis of cochlear emissions has relied on a "dual-component" theory. The conceptual framework for the theory and the quantitative description that builds upon it are based on cochlear wave mechanics, in which both forward and reverse cochlear traveling waves are present (Kemp, 1986; Zweig and Shera, 1995; Talmadge *et al.*, 1998; Shera and Guinan, 1999). The theory predicts that after being generated by nonlinear outer hair cell forces, a DP will travel as a cochlear traveling wave in reverse to emerge as a DPOAE (as a "generator" or "wave-fixed" component). In a scaling-symmetric cochlea the amount of phase accumulation to the generation place (where f_2 and f_1 have substantial overlap) is approximately unchanged as the primary frequencies are swept (at a fixed ratio). Therefore the phase of the generator component of the DPOAE is not expected to change with frequency when f_1 and f_2 are swept at fixed ratio (Shera *et al.*, 2000). In addition, irregularities in the cochlea's sensory tissue will give rise to reflections of the DP. The largest reflector contributions will come from close to the DP's BF place, where the DP will be large due to cochlear filtering and amplification. The reflected wave will contribute to the DPOAE (as a "reflector" or "place-fixed" component). In the dual-component theory, amplitude fine structure is due to interference between the generator and reflector components (e.g., Stover *et al.*, 1996; Talmadge *et al.*, 1999; Kalluri and Shera, 2001). Because the phase of a single tone changes rapidly in the region of its own BF place, the phase of the reflector component of the DPOAE changes rapidly with frequency. In this description, the slope of the phase-frequency response (group delay) of the reflector component at a given frequency is expected to be roughly twice the group delay of a single tone at the intracochlear BF region corresponding to

that frequency. The dual-component theory, and the separation of the observed emissions into reflector and generator emission types, was found to provide a useful framework for the interpretation of some of our results. This separation is aided by the fixed-ratio stimulus paradigm (as opposed to fixed f_1 or fixed f_2) (Knight and Kemp, 2000; Shera *et al.*, 2000; Kalluri and Shera, 2001; Knight and Kemp, 2001) and therefore we use this paradigm most extensively.

In order to use emissions to study the cochlea we must first understand if and how they are shaped as they travel out through the middle ear. The study of Avan *et al.* (1998) related DPs measured close to the stapes to DPOAEs to quantify middle-ear reverse transmission in the guinea pig. Similarly, Dong and Olson (2006) compared intracochlear DPs close to the stapes to DPOAEs to quantify middle-ear reverse transmission in the gerbil. The main result of that study, which will be required for the present study (also in the gerbil), was that the middle ear did not introduce very much structure into the emissions but, like forward transmission (Olson, 1998), had a fairly flat transfer function at a level of $\sim$−40 dB (compared to the $\sim$+25 dB forward gain of the middle ear) and a phase that was delaylike with a delay of $\sim$38 μs (slightly longer than the $\sim$32 μs forward delay). The delaylike character of middle-ear transmission both in the forward and reverse directions is a robust finding; inter-animal variability in delay time was small and could be attributed to the location of the microphone probe tube within the EC. Superimposed on this simple description, fine structure in the reverse transfer function was present at the $\pm$5–10 dB level in the amplitude, and at the $\pm$20°–30° level in phase and appeared to be linked to the acoustic load of the speaker and microphone system. Scala Vestibuli (SV) pressure was not measured in the present study. Therefore, the average middle ear forward and reverse phase responses from Dong and Olson (2006) are presented in many of the figures in order to illustrate the contribution of the middle ear to the observed phase behavior.

There have been just a handful of joint DP and DPOAE measurements that were designed to probe the intracochlear travel of DPs. Cooper and Shera (2004) compared DPOAE and DP phase-frequency responses measured in the same guinea pig (sequentially in time), and showed that the results were consistent with the reverse-traveling wave: the phase-frequency slope (group delay) of the DPOAE at frequencies close to the BF of the intracochlear measurement location was approximately twice the group delay of a BF tone, measured within the cochlea. This result indicated that the travel time out of the cochlea was similar to the travel time in. Another emission type (stimulus frequency emission) was also measured and led to the same conclusion. In addition, the study showed that the amplitude of the DP response in BM motion was tuned in frequency but that at frequencies below the BF it contained amplitude notches not present in the tuning of the primaries. This behavior was also observed in our previous DP studies (Dong and Olson, 2005b, a; Olson and Dong, 2006). The behavior is predicted due to destructive interference between locally or basally generated distortion and apically generated distortion, traveling out of the cochlea through the base. These results supported the existence of reverse-traveling waves.

However, the results of some intracochlear measurements call into question the existence of the reverse-traveling wave. Measurements of BM motion that extended for $\sim$1 mm in the longitudinal direction were used to look for the reverse-going wave (Ren, 2004; He *et al.*, 2007). DP cochlear traveling waves were detected, but their spatial–temporal character indicated that they were traveling in the forward direction. Moreover, the delay calculated with the phase-frequency slope of the DPs measured at the stapes (a proxy for the DPOAEs) was shorter than that of the DP on the BM. The interpretation of those results was that the DP traveled out of the cochlea to the stapes directly through the cochlear fluid as a (fast) compression pressure, and stapes excitation by the DP launched a forward-traveling wave. The possibility for a role of compression pressure in emissions is supported by the presence of emissions in animals such as frogs that lack a clear traveling wave (Wilson, 1980; van Dijk and Manley, 2001; Ruggero, 2004). However, in the mammalian cochlea the basic mechanics for reverse cochlear traveling waves is the same as for forward waves (flexible sensory tissue coupled to fluid inertia) and it is reasonable to expect that in mammals DPs would primarily travel out as a reverse wave—unless something about the sensory tissue's cellular architecture suppresses reverse waves. For sure, the fact that an experiment designed to directly observe a reverse cochlear traveling wave (Ren, 2004; He *et al.*, 2007) failed to do so has reinvigorated the compression DP theory.

The manner in which distortion products, and emissions in general, emerge from the cochlea is important for two prominent reasons. First, basic models of cochlear mechanics allow reverse waves, and their absence (or very small size) would point to a directional advantage for forward-going waves. This restriction would constrain cochlear models. Second, as noted above, cochlear group delays have been correlated with tuning. If emission phases are used to gauge intracochlear group delays it is important to know if the phase accumulation that is used in the group delay calculation reflects forward and reverse travel, or just forward travel. In this contribution we weigh in on the reverse wave/compression wave question. We simultaneously measured intracochlear pressure DPs both close to and far from the BM and DPOAEs. We first describe relevant aspects of the DPOAE and DP frequency responses individually. Then we relate the DPOAEs to the DPs to explore their relationship to one another. In particular, we explore their relative phase behaviors as this can be examined for a reverse-traveling-wave character.

II. METHODS

A. Animal preparation

The gerbil audiogram extends to $\sim$50 kHz (Ryan, 1976) and the BF of our intracochlear location was $\sim$20 kHz. Animal procedures were approved by the Institutional Animal Care and Use Committee of Columbia University. The experimental animals were young adults, 50–70 g. The gerbils

were deeply anesthetized throughout the experiment and euthanized at the end. (Forty milligrams per kilogram ketamine was administered first to sedate the animal, then an initial dose of 60 mg/kg sodium pentobarbital, with supplemental doses of 10 mg/kg for maintenance of deep anesthesia. Twenty mg/kg of the analgesic buprenorphine was administered every 6 h. At the end of the experiment the animal was overdosed with sodium pentobarbital.) A tracheotomy was performed to maintain a patent airway. The animal core temperature and head holder were maintained at ~37 °C with a heating blanket and a power resistor on the head holder. The left bulla was widely opened with great care to access the cochlea. A small hole (diameter ~200 μm) was hand drilled through the bony wall in the basal-turn scala tympani (ST). To gauge cochlear health, the compound action potential (CAP) thresholds and DPOAE were recorded with a silver electrode at the round window and EC several times during the experiment, in particular before and after making the ST hole.

B. Sound stimulation and data acquisition

The ear was acoustically stimulated via a single Radio Shack 40-1377 tweeter coupled to the ear canal in a closed-system configuration. Acoustic stimuli were generated and collected digitally using Tucker Davis Technologies System 3. One- and two-tone stimuli were used in the experiments. The single tone was swept from 0.2 to 50 kHz with frequency spacing of 500–1000 Hz, at stimulus levels from 40 to 90 dB SPL. For two-tone stimuli, two equal-intensity primary tones were delivered at a fixed f_2:f_1 ratio, 1.05 or 1.25, and f_1 and f_2 were swept in frequency with an f_2 frequency spacing of 100–400 Hz or f_2 was fixed at BF and the f_2:f_1 ratio was varied by sweeping f_1. Frequency sweeps were useful because the responses could be examined for tuning and for a traveling-wave-like phase. For the constant f_2:f_1 ratio paradigm, the overlapping pattern of the responses to the primaries was maintained approximately constant and simply moved longitudinally along the organ of Corti as the stimulus frequencies were swept, as described and motivated in Sec. I.

The sound pressure level was calibrated in the EC within 3 mm of the tympanic membrane using a Bruel & Kjaer probe-tube microphone system (Sokolich, 1977). The frequency-dependent transfer function of the probe tube was accounted for when setting the sound pressure level and analyzing the data. This microphone also served as the receiver of otoacoustic emission pressure, as described previously (Dong and Olson, 2006). Data acquisition times were either 0.4 or 1 s for individual stimulus sets. The longer time was used with some of the low level stimuli to increase the signal-to-noise ratio. The noise level indicated in the figures was determined by taking the average of the microphone voltage spectra recorded during data collection, after removing the prominent peaks at primary and $2f_1-f_2$ and $2f_2-f_1$ DP frequencies. The source of noise is photon shot noise in the case of the sensor, and electronic noise in the case of the probe microphone system, and both are flat in frequency. The voltage noise was converted to equivalent pressure noise using sensor and microphone voltage-to-pressure conversions. The microphone conversion is not flat with frequency, and so the noise level of the microphone expressed in pressure exhibits mild frequency structure. With 1 s data acquisition time its noise level was ~5–10 dB SPL up to 30 kHz, and slightly higher at higher frequencies. In order to measure the DPOAE over a wide frequency range with equal-intensity primary tones, the stimulus level needed to be above 60 dB SPL. The noise floor of our intracochlear pressure measurement is 50–60 dB SPL, and the DP was typically above this level only with primary levels at least 60 dB SPL. Therefore, for the study of distortion products, both our intracochlear and ear canal pressure measurement systems limit us to stimulus levels above ~60 dB SPL. Measurements made at lower levels would extend these studies and offer further information about some of the key issues. However, distortion generated with relatively high sound stimuli likely has the same basic origin (cochlear outer hair cells) as low level distortion (Kim *et al.*, 1980; Lukashkin *et al.*, 2002; Mills, 2002; Avan *et al.*, 2003), and we will show below that its tuning and physiological fragility are consistent with this view. Acoustic distortion was checked in a cavity and was at least 70 dB beneath the level of the primaries when the primary level was 100 dB SPL, and smaller for lower primary levels (Dong and Olson, 2005b), so artifactual distortion did not influence our results.

The design, construction, and calibration of the fiber-optic pressure sensor has been described (Olson, 1998). The sensors used in the present study were 150 μm in outer diameter, slightly smaller than the 167 μm outer diameter of the original design. The sensors operate with wide band sensitivity (Pa/V) that is flat to within a few decibels to at least 50 kHz. The sensitivity can change due to small adjustments of the sensitive membrane. Therefore, the absolute sensitivity is known to ~±10 dB. An individual sensor tip might be used in several experiments or just one if the sensitive membrane was damaged. They were positioned close to the BM in the basal-turn ST of the cochlea (BF~20 kHz) by advancing in micrometer steps with a stepper motor. The distance to the BM was judged by tapping it, whereupon a noisy low-frequency signal was observed on the monitor oscilloscope. Most of the measurements were made close to the sensory tissue, but sometimes additional measurements were made at various distances from the BM. The question of whether the sensor perturbed cochlear mechanics is salient. It has been explored previously (Olson, 2001) and below we explore it further.

C. Phase calculation

When considering ST primary or single-tone pressure responses to the EC stimulus, the phase is simply referenced as

$$\phi_{\text{ST-re-EC}} = \phi_{\text{ST}} - \phi_{\text{EC}}$$

(at primary or single-tone frequencies).

When considering the DPOAE in the EC as a response to the DP in ST (when looking for a reverse wave), the phase is simply referenced as

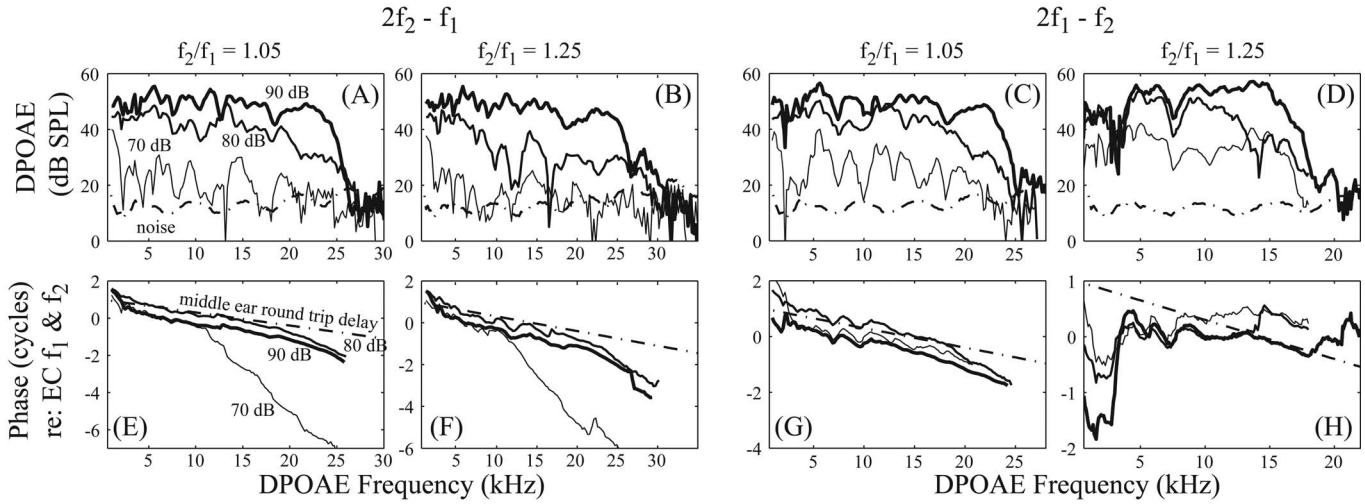

FIG. 2. The $2f_1-f_2$ and $2f_2-f_1$ components measured from an ear with intact cochlea showing the complex nature of the DPOAE. The bulla was open for measuring CAP thresholds at the round window and the cochlea was intact. (A) and (B) The $2f_2-f_1$ amplitude with $f_2:f_1$ ratio of 1.05 and 1.25. (C) and (D) The $2f_1-f_2$ amplitude with $f_2:f_1$ ratio of 1.05 and 1.25. Dotted–dashed line shows the noise floor of the B & K probe-tube microphone. (E)–(H) DPOAE phase referenced to f_1 and f_2 phases in the EC. Dotted–dashed line shows the average middle-ear round-trip delay from Dong and Olson (2006). The two primaries were equal intensity of 70 (thin line), 80 (medium), and 90 dB SPL (thick). $f_2:f_1$ ratio was fixed either at 1.05 or 1.25. f_2 swept from 1000 to 30 000 Hz in 200 Hz steps (animal wg92).

$$\phi_{\text{EC-re-ST}} = \phi_{\text{EC}} - \phi_{\text{ST}} \quad \text{(at DP, DPOAE frequencies)}.$$

Because the DP frequencies are not contained in the stimulus, to reference the DP or DPOAE to the stimulus in the EC requires the following (Dong and Olson, 2005b, 2006), where ϕ_{ECf1} and ϕ_{ECf2} are the phases of the EC primaries:

$$\phi_{2f1-f2\text{-re-EC}} = \phi_{2f1-f2} - (2\phi_{\text{ECf1}} - \phi_{\text{ECf2}}) \quad (2f_1 - f_2 \text{ DP or DPOAE}),$$

$$\phi_{2f2-f1\text{-re-EC}} = \phi_{2f2-f1} - (2\phi_{\text{ECf2}} - \phi_{\text{ECf1}}) \quad (2f_2 - f_1 \text{ DP or DPOAE}).$$

In order to account for the phase behavior that is attributable to middle-ear transmission we use the average middle-ear transmission delays observed in Dong and Olson (2006). The phase versus frequency due to middle-ear forward transmission is found as $(-1)\times$frequency $\times$the forward delay of 32 μs. Similarly, the phase versus frequency due to middle-ear reverse transmission and round-trip transmission are found, respectively, as $(-1)\times f \times 38$ μs (the reverse delay) and $(-1)\times f\times 70$ μs (sum of forward and reverse delays). The forward and reverse middle-ear delay times are similar and in some cases the small difference between them is neglected.

III. RESULTS

Seventeen animals contributed to this study. All these animals were preparations with robust nonlinear tuning, nonlinear responses, and starting healthy CAP thresholds. Results from individual animals are shown to illustrate particular points, and grouped data show the generality of the results. Animal wg96 is an important case because some of the DP and DPOAE data were collected with the sensor close to the BM but before tapping it, so these results inform questions about sensor perturbation. Because tapping did not affect the results in wg96, the data from this experiment are also representative of other animals in which tapping occurred prior to most data collection.

A. Basic characteristics of DPOAEs and DPs

1. DPOAEs are complex

In Fig. 2 we show DPOAEs produced with equal-intensity primary levels of 70, 80, and 90 dB SPL in a gerbil with an intact, unopened cochlea. The amplitudes of the $2f_1-f_2$ and $2f_2-f_1$ DPOAE components are in panels 2(A)–2(D), their phases relative to the primaries (f_1,f_2) in the EC are in panels 2(E)–2(H). The DPOAE was level, frequency, and ratio dependent. The DPOAE was observable up to 20–30 kHz, and then dropped to the noise floor. The $2f_1-f_2$ and $2f_2-f_1$ amplitudes were similar with a $f_2:f_1$ ratio of 1.05 [Figs. 2(A) and 2(C)], while the $2f_1-f_2$ was bigger than $2f_2-f_1$ with a $f_2:f_1$ ratio of 1.25 [Figs. 2(B) and 2(D)], especially at the lower primary levels. The DPOAE generally grew with increasing primary level. In general, the DPOAEs elicited with moderate level primaries [e.g., 70 dB data in Figs. 2(A)–2(D)] displayed more fine structure than DPOAEs elicited with high level primaries. The phase of $2f_2-f_1$ changed rapidly with frequency above 12 kHz with the 70 dB SPL primary level [Figs. 2(E) and 2(F)]. In the region of the rapidly varying phase, this DPOAE would be interpreted as a place-fixed, reflector emission. The phase-frequency response of the $2f_1-f_2$ component at a wide $f_2:f_1$ ratio of 1.25 was flat through a fairly broad frequency range [Fig. 2(H)]. The flat phase is associated with the wave-fixed emission type. Because the middle ear round-trip delay is unavoidable, within the cochlea the phase-frequency response must actually slope upward (by simple subtraction of phase slopes), and we will see in what follows that this is in fact the case. The phase of the DPOAE was in other cases very much like the round-trip middle ear delay [Figs.

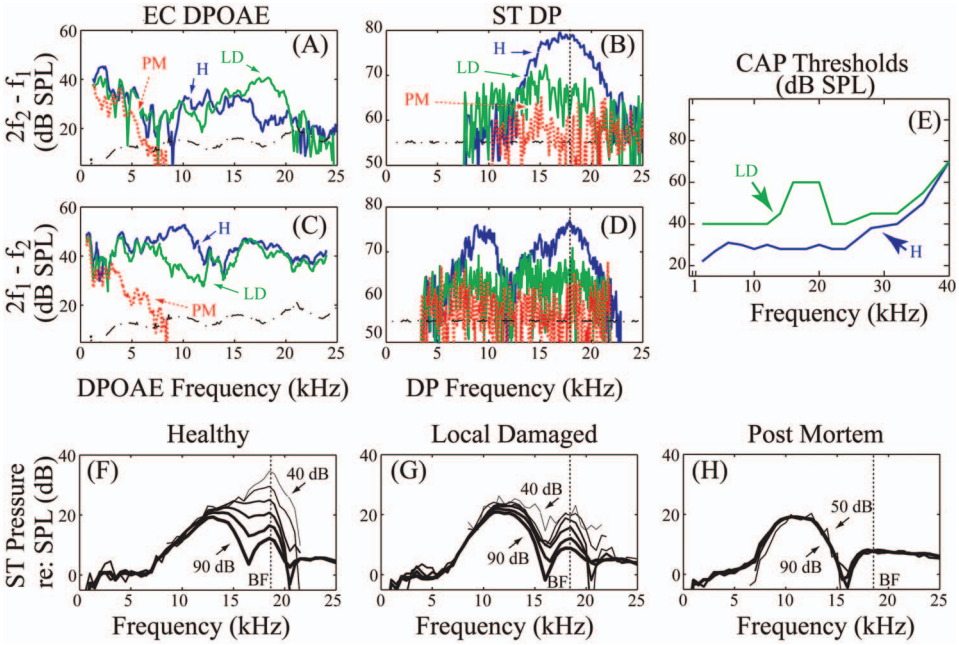

FIG. 3. Simultaneous recording of DPOAE in the EC and DP in the ST close to the BM with different cochlear conditions: healthy (H) (blue), locally damaged (LD) (green), and postmortem (PM) (red). The pressure sensor was positioned ~10 μm from the BM at the basal turn of the cochlea with BF ~18 kHz. (A) and (C) DPOAE $2f_2-f_1$ and $2f_1-f_2$. (B) and (D) DP $2f_2-f_1$ and $2f_1-f_2$. ($L_1=L_2=80$ dB SPL, $f_2:f_1=1.25$, f_2 swept from 1000 to 40 000 in 100 Hz steps.) (E) CAP thresholds under healthy and locally damaged conditions. (F)–(H) Single-tone amplitude responses (normalized to SPL) from the same position/conditions with stimulation levels of 40–90 dB SPL in 10 dB steps. Vertical dotted line indicates the BF position. Single-tone nonlinearity and local DPs were severely reduced with damage and the CAP thresholds were elevated, especially in the frequency region of damage (B), (D), (E), and (G). Postmortem, single-tone responses became linear and the DPs were reduced almost to the noise level (B), (D), and (H). DPOAEs changed over a limited frequency region due to local damage, and were greatly reduced postmortem (A), (C) (animal wg95).

2(E)–2(G)], although often with a superposed jagged structure that lined up with ripples in the magnitude. After accounting for the middle ear round-trip phase, the cochlear phase-frequency response would be flat, and in the dual-component emissions theory, this emission type would also be interpreted as a type of wave-fixed emission.

2. Local damage reduces DPs and changes DPOAEs, death reduces both dramatically

Because we worked at relatively high stimulus levels, it is important to demonstrate the physiological basis of the DPs and DPOAEs we measure. Figure 3 shows how the simultaneously recorded DPOAE [Figs. 3(A) and 3(C)] and DP [Figs. 3(B) and 3(D)] changed due to local damage and death. The cochlear condition is illustrated by CAP thresholds [Fig. 3(E)] and the ST pressure responses measured close to the BM with single-tone stimuli [Figs. 3(F)–3(H)]. The $2f_1-f_2$ and $2f_2-f_1$ are plotted versus their own frequencies, under intact cochlea (blue), local cochlear damage (green), and postmortem (red) conditions.

Before damage, the CAP measurements showed a typical threshold curve, with thresholds about 30 dB SPL up to 24 kHz, and then growing with frequency [Fig. 3(E)]. The single-tone responses showed saturating nonlinearity [Fig. 3(F)]. The BF of this position (peak frequency at low stimulus level) was ~18 kHz. The $2f_2-f_1$ DP was tuned approximately to the BF [Fig. 3(B)] and the $2f_1-f_2$ DP had two peaks [Fig. 3(D)], which will be discussed further in regard to Fig. 5. The DPOAE was broadband, with notches [Figs. 3(A) and 3(C)]. After using the sensor to cause local permanent damage to the organ of Corti, CAP thresholds were elevated at all frequencies except for the highest tested with a pronounced elevation in the 16–21 kHz region [Fig. 3(E)]. (In this experiment the sensor was inadvertently bumped and the local damage technique was not well controlled. We have reproduced elements of this response to localized damage in other experiments by distending the BM with the sensor by ~10 μm.) In addition, the single-tone response gain and degree of nonlinearity was reduced (but not eliminated), indicating that the cochlea's active nonlinear mechanics were damaged [Fig. 3(G)]. At frequencies far from the BF the changes were small and the similarity with predamage values shows that the sensor itself was not damaged when it was used to damage the organ of Corti. The DPs [Figs. 3(B) and 3(D)] were markedly reduced at peak frequencies, and less reduced at frequencies on the low side of the peaks. This applies to both peaks in Fig. 3(D). The DPOAEs [Figs. 3(A) and 3(C)] were only substantially affected in the frequency region corresponding approximately to the BF of the damaged region [slightly below the BF region in Fig. 3(C)]. The $2f_1-f_2$ DPOAE [Fig. 3(C)] decreased; the $2f_2-f_1$ DPOAE [Fig. 3(A)] actually *increased*. This might be because the local damage caused the sensory tissue to be less smooth, enhancing the reflection of DPs. In the postmortem condition, the single-tone responses became linear [Fig. 3(H)], the DPs went into the noise [Figs. 3(B) and 3(D)], and the DPOAEs went into the noise at frequencies above ~7 kHz [Figs. 3(A) and 3(C)]. At frequencies below 5 kHz the DPOAEs remained robust in these data, taken ~30 min postmortem. In other animals, more than 1 hour postmortem the DPOAE disappeared beneath the noise floor even at a stimulus level of $L_1=L_2=90$ dB SPL. In sum, this figure illustrates that the DPOAEs and DPs are both sensitive to localized damage and death and that the DPOAE is sourced by intracochlear distortion even at high stimulus levels.

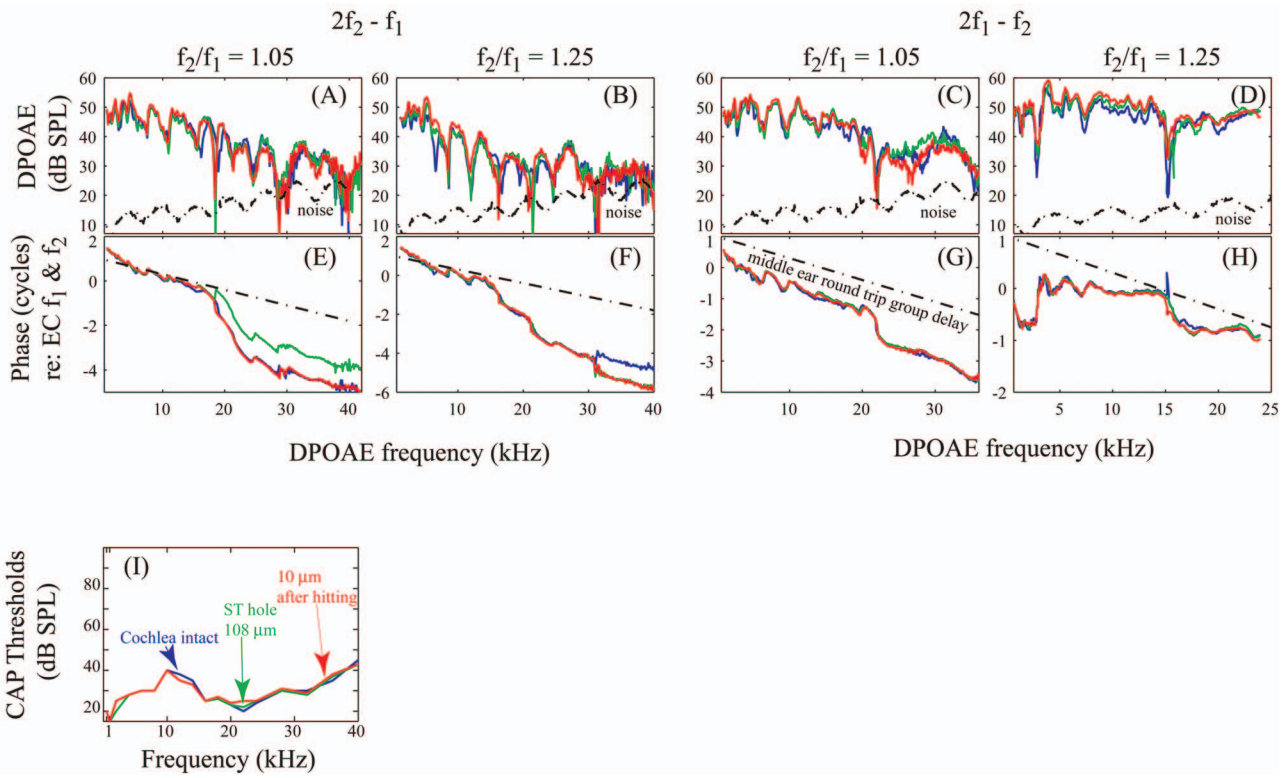

FIG. 4. Lack of sensor perturbation to DPOAE and CAP thresholds. (A)–(D) $2f_2-f_1$ and $2f_1-f_2$ DPOAE amplitude. Dotted–dashed lines indicate the B & K probe-tube microphone noise floor in the EC. (E)–(H) $2f_2-f_1$ and $2f_1-f_2$ DPOAE phase relative to EC f_1 and f_2 phases. Dotted–dashed lines represent the middle-ear round-trip delay. (I) CAP thresholds. Blue lines show data collected with the cochlea intact. Green lines indicate responses with the ST hole and sensor at 108 μm from BM and red lines represent data with the sensor 10 μm from BM after tapping it. The primary stimuli were equal-intensity tones of 80 dB SPL with $f_2:f_1$ ratio fixed at either 1.05 or 1.25. f_2 frequency was swept from 1000 to 40 000 Hz in steps of 100 Hz. The DPOAE and CAP thresholds were nearly unchanged after making the ST hole, introducing the sensor into ST, and after tapping the BM (animal wg96).

3. Introducing the sensor into the cochlea does not perturb cochlear mechanics

The micropressure sensors have been used for nearly a decade to explore cochlear mechanics (Olson, 1998, 1999, 2001, 2004; Dong and Olson, 2005b, a; Olson and Dong, 2006; Decraemer *et al.*, 2007). In previous studies, the presence of the sensor close to the BM sometimes caused the CAP threshold to be elevated a few decibels and in other cases had no effect on CAP (Olson, 2001, Fig. 6). To further explore the possibility that the presence of the pressure sensor perturbs cochlear mechanics, DPOAEs and CAP thresholds are plotted in Fig. 4 under three different conditions: prior to opening the cochlea (blue), after making the sensor hole and positioning the sensor within the cochlea before using it to tap the BM (green), and after hitting the BM and withdrawing 10 μm (red). Changes to the DPOAE [panels 4(A)–4(H) and CAP [panel 4(I)] were barely discernible, and could be due to slight repositioning of the acoustic system. The most pronounced change, in the phase of the low ratio 1.05 $2f_2-f_1$, is tied to the deep notch at ~20 kHz and phase unwrapping, as after they have diverged, the green, and red and blue curves differ by a complete cycle. In summary, Fig. 4 illustrates lack of sensor perturbation. Therefore, unless noted, the data presented here are expected to reflect normal cochlear mechanics.

B. Further characteristics of the DP

The characteristics of locally measured DPs help us to understand their relationship to DPOAEs. In Dong and Olson (2005b, a) and Olson and Dong (2006), locally measured intracochlear DPs at a low $f_2:f_1$ ratio (1.05) were explored in some detail. At frequencies close to the local BF the DPs were tuned and showed similar group delays to the primaries, suggesting they were locally or basally generated. However, at frequencies somewhat below the BF, the group delays were longer than those of the primaries, which indicated nonlocal DP generation. Here, we also show DP results taken with the paradigm with a relatively high $f_2:f_1$ ratio (1.25) to further our understanding of intracochlear DPs.

1. Variations with frequency indicate that DPs are composed of a combination of locally and distantly generated components

Figure 5 shows the $2f_1-f_2$ DP in ST pressure measured close to the BM from wg93. The stimuli were equal-intensity tones of 70, 80, and 90 dB SPL (blue, green and red). The high level results are the most extensive (out of the noise), and 70 dB data extend the results to moderate stimulus levels. The responses are plotted versus the DP frequency in panels 5(A) and 5(B) (amplitude) and panels 5(C) and 5(D) (phase relative to EC f_1 and f_2 primary phases). The amplitude data are replotted versus f_2 in panels 5(E) and 5(F). Single-tone tuning curves and phase are plotted as dotted lines, for comparison.

The low ratio 1.05 data [Fig. 5(A)] show tuning that was much like single-tone tuning in the region of the peak. With primary levels of 70 dB the response was tuned much like

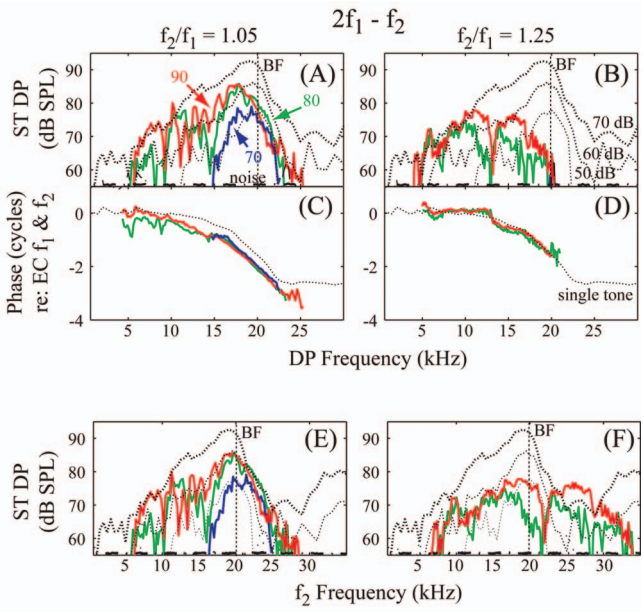

FIG. 5. Scala tympani $2f_1-f_2$ DP amplitude and phase show both locally/basally and remotely generated components. Sensor was positioned 10 μm from the BM, $L_1=L_2=70$, 80, and 90 dB SPL. $f_2:f_1$ was fixed at either 1.05 or 1.25. f_2 was swept from 1000 to 35 000 in 200 Hz steps. (A) and (B) Amplitude of the $2f_1-f_2$ DP with $f_2:f_1$ ratio of 1.05 and 1.25, respectively. (C) and (D) Corresponding phase, referenced to the EC primaries. In (A)–(D) DPs are plotted vs their own frequency. (E) and (F) DP amplitude is plotted vs the f_2 frequency, to better understand the basis for tuning. Solid colored lines show the DP responses; dotted lines show single-tone pressure responses at 50, 60, and 70 dB SPL, measured at the same position, for comparison. Dotted–dashed lines show the noise floor of the sensor and vertical dotted line indicates the BF position (animal wg93).

the 50 dB SPL single-tone response. With primary levels of 80 and 90 dB the peak was shifted to slightly lower frequencies. This shift suggests that the tuning of the DPs resulted from both primary tuning (pregeneration) and DP tuning postgeneration. We pursue this by plotting the DP versus f_2 frequency in Fig. 5(E). The single-tone curve was slightly better fit in Fig. 5(E) than in Fig. 5(A) (at the higher sound levels), supporting the idea that the DP tuning was substantially influenced by primary tuning. In the region of the peak the phase versus DP frequency was much like the single-tone response [Fig. 5(C)], indicating a forward-traveling DP. Below 15 kHz, the DP amplitude showed features that are reminiscent of DPOAE fine structure [Figs. 5(A) and 5(E)]. In this sub-BF frequency region the phase [Fig. 5(C)] departed from the single-tone behavior; it was steeper, and more structured. Thus, the amplitude and phase of the low-frequency DP make it clear that it is not purely locally/basally generated and it is likely that apically produced distortion is contributing.

The high ratio 1.25 $2f_1-f_2$ DPs (right panels) were not tuned like the single tone when plotted versus the DP frequency. Because at high ratio (1.25) the primary and DP frequencies are much more separated than with the low ratio (1.05) condition, it is to be expected that the DP tuning would be more complicated. In Fig. 5(B) two well defined peaks were apparent in the amplitude and correspond to flat (lower-frequency peak) and single-tonelike (higher-frequency peak) phase responses, respectively [Fig. 5(D)]. The dual-peak structure was also observed in other animals [e.g., Fig. 3(D)]. The higher-frequency peak likely corresponds to basally produced distortion traveling forward, but it is curious that it cuts off at frequencies below the BF. When plotted versus f_2 (Fig. 5(F)) it is seen that the second peak extends to f_2 frequencies above 30 kHz. Frequencies of 30 kHz and above are represented in the basal region of the gerbil cochlea that is exposed by the large round window opening. It is possible that in this open cochlea the basal region is beginning to deteriorate (Overstreet *et al.*, 2003). This could account for the second peak's premature high-frequency dropoff compared to the single-tone response in Fig. 5(B). With this understanding, the second peak is convincingly a forward-traveling DP. The lower-frequency peak had a flat phase [Fig. 5(D)], which was similar to the DPOAE response typically observed for the $2f_1-f_2$ component at a high ratio (1.25) [Figs. 2(H) and 4(H)]. In fact, the sub-BF frequency phase was not flat, but sloped slightly upward. When describing the flat $2f_1-f_2$ phase with the $f_2:f_1$ ratio of 1.25 in Fig. 2 we predicted this type of upward sloping DP phase in order to account for both the flat DPOAE phase and the middle-ear delay. The lower-frequency peak at the 90 dB stimulus level in Fig. 5(F) was tuned somewhat like the single-tone f_2 response, but the correspondence is less clear at the 80 dB stimulus level. The sharp notch separating the low- and high-frequency peaks suggests interference, such as would occur if locally and remotely generated components were summing destructively. In sum, the lower-frequency peak in Figs. 5(B) and 5(F) appears to be a combination of locally generated distortion (or basally generated distortion that traveled forward) and distantly generated distortion, traveling out of the cochlea from more apical locations.

2. Spatial variations show that the DPs drop off steeply with distance from the BM

Intracochlear pressure is composed of compression and traveling-wave modes. In Sec. I we described how these appear in measurements; a review point is that the traveling-wave mode is dominant close to the BM at frequencies close to BF and diminishes rapidly with distance from the BM, whereas the compression mode is dominant far from the BM or at frequencies higher than the BF, and is not spatially varying. In Fig. 7 of Dong and Olson (2005b) we showed that DP pressures decreased with distance from the BM. Here we confirm this finding. Figures 6(A) and 6(A′) show the $2f_2-f_1$ DP when the sensor was far from the BM (thin lines) and close to it (thick lines). For comparison, the f_2 primary response at these locations is also plotted [Figs. 6(B) and 6(B′)] The response phases (both f_2 and DP) are shown in Figs. 6(C) and 6(C′). We also show the concurrently measured DPOAE in Figs. 6(D) and 6(D′). The DPOAE changes were small, suggesting that the sensor's location did not influence cochlear mechanics, and confirming the results from Fig. 4. The f_2 amplitude was bigger at the closer than it was at the more distant location, with the largest changes in the region of the BF peak. (Based on low intensity single-tone tuning curves the BF was ~18 kHz for wg95 and 21 kHz for wg92.) The notches in the primary amplitude [arrowheads in

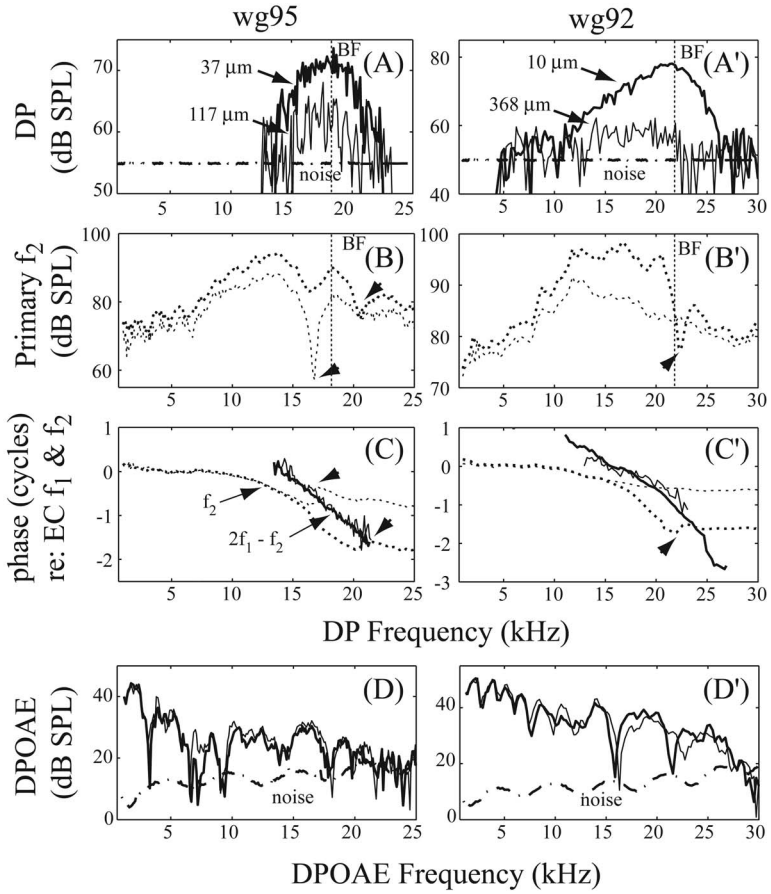

FIG. 6. DP spatial variation shows that the DP drops off with distance from the BM. (A) and (A′) $2f_2-f_1$ DP amplitude measured at distances far (thin) and close (thick) to the BM. Dotted–dashed lines indicate the sensor noise floor. Vertical dotted lines represent the BF position. (B) and (B′) Amplitude of primary f_2 measured close to (thick dotted) and far from (thin dotted) the BM. (C) and (C′) Phase referenced to EC f_1 and f_2. DP and primary f_2 responses are plotted in solid and dotted lines, respectively. Arrowheads indicate frequency/position combinations for which destructive interference between compression and traveling modes is apparent. (D) and (D′) Concurrently measured DPOAE is stable, indicating a lack of significant sensor perturbation. ($L_1=L_2=80$ dB SPL, $f_2:f_1=1.25$, f_2 swept in 100 Hz (animal wg95) or 200 Hz (animal wg92) steps). The DP decreased as the distance from the BM increased, similar to the primary response in the BF frequency region.

Figs. 6(B) and 6(B′)] coincide with phase jumps [arrowheads in Figs. 6(C) and 6(C′)], and are due to destructive interference between traveling- and compression wave pressure modes. At frequencies well above the BF, the compression wave dominated the f_2 responses, which led to the phase and amplitude plateaus. When the sensor was positioned far from the BM the region of compression wave dominance started at a lower frequency [phase plateau region thin-dotted versus thick-dotted lines in Figs. 6(C) and 6(C′)]. The phase plateaus at the different locations are separated by a full cycle. Over much of the frequency range, the DP phase lined up with the forward-traveling f_2 phase (so the DP is also forward traveling, or locally generated). However, in Fig. 6(C) and 6(C′) at frequencies less than 15 kHz, the DP phase was steeper than the primary phase, suggesting that in this region, apically generated distortion traveling backward was contributing to the measured DP.

Most importantly, the DP amplitude decreased substantially with distance from the BM [Figs. 6(A) and 6(A′)]. The rapid spatial variations in the DP prove that it is not a compression pressure, since the observed pressure differences must drive bulk acceleration of the cochlear fluid. The spatial variations observed in the DPs are similar to those of the traveling-wave pressure mode of the primary response, which argues for a traveling-wave mode of DP travel. In general, the DP steadily dropped to the noise level as the measurement position was moved further from the BM. Therefore, the noise level (~55–60 dB SPL) gives the upper limit for the size of a compression-type (approximately space-filling) DP pressure.

C. Relating DPOAEs to DPs

A robust feature of cochlear mechanics is the phase-frequency relationship of the forward-traveling wave, illustrated in Fig. 1(C). Therefore, a very compelling demonstration of a reverse-traveling wave would be the observation of the same phase-frequency relationship, in reverse. The forward-traveling-wave phase is found by referencing the intracochlear response to the EC stimulus and the reverse-traveling phase can be sought by referencing the EC emission to the intracochlear DP. If this DPOAE–DP phase overlies the forward-traveling-wave phase, the reverse-traveling wave will be supported. In the following figures, we show the result of this referencing. We will find that the DPOAE–DP phase results cannot stand on their own definitively, but that coupled with the individual DP and DPOAE results, compelling conclusions can be drawn.

Figures 7–10 show the simultaneous measurements of DPOAE and DP in animals wg81 and wg96. The amplitude and phase of $2f_2-f_1$ DPOAE and DP are in panels (A)–(D); amplitude and phase of $2f_1-f_2$ DPOAE and DP are in panels (F)–(I); the DPOAE–DP phase is in panels (E) and (J)—it is this plot that will be explored for a reverse-traveling-wave character. DPs in these figures were measured close to the BM (within 30 μm). For comparison/reference, average middle-ear round-trip delay is plotted in panels (B) and (G) (dotted–dashed lines) and middle-ear reverse transmission delay is plotted in panels (E) and (J) (dotted–dashed line). The single-tone phase response to a 50 dB SPL stimulus tone from the same experimental animal and conditions as the DP,

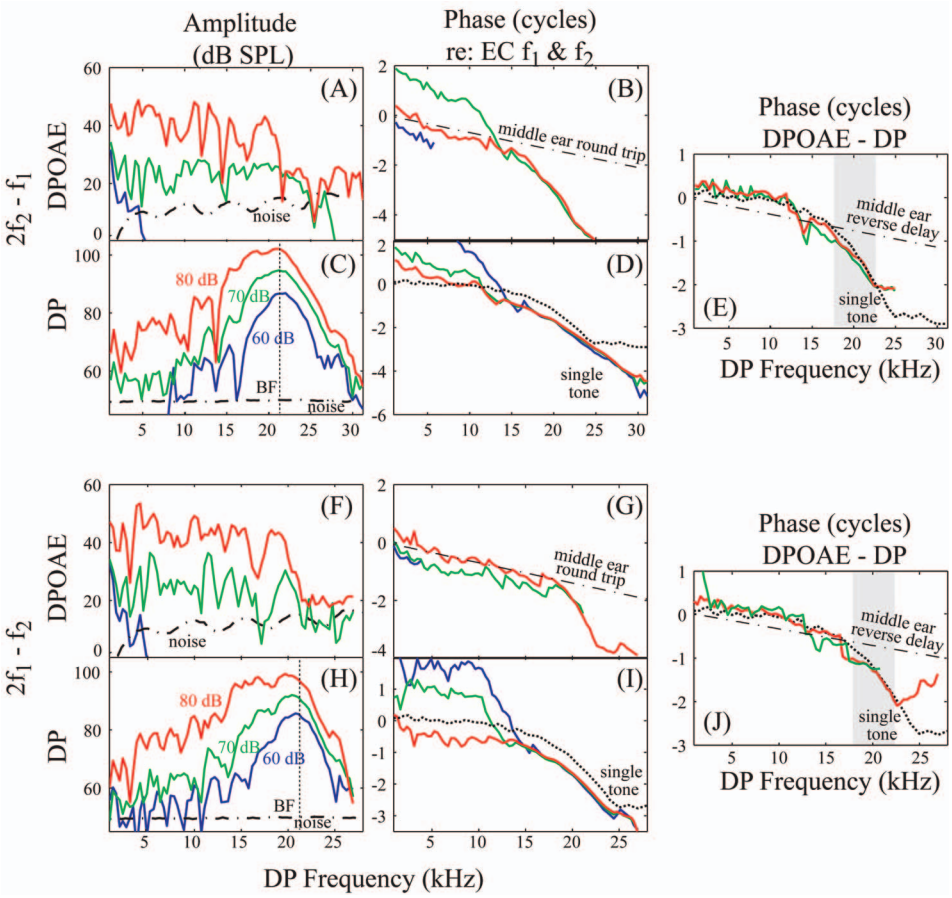

FIG. 7. Simultaneous recording of the DP and DPOAE with $f_2:f_1=1.05$. $L_1=L_2=60$ (blue), 70 (green), and 80 dB SPL (red), the sensor was positioned 20 μm from BM. f_2 was swept from 1000 to 40 000 in 400 Hz steps. (A), (C), (F) and (H) The $2f_2-f_1$ and $2f_1-f_2$ DP and DPOAE amplitudes. Dotted–dashed lines indicate the noise floor of the sensor and B and K probe-tube microphone. Vertical dotted lines represent the BF position. (B), (D), (G) and (I) Phases of DP and DPOAE referenced to EC f_1 and f_2 phases. Dotted–dashed lines show the middle-ear round-trip delay and dotted lines show the single-tone forward-traveling-wave phase, for comparison. (E) and (J) Phase of the DPOAE referenced to the DP phase. When this phase overlaid the forward-traveling wave of the single tone, the reverse wave is considered to be detected. Within the BF frequency region (gray bar), the observation of the reverse wave depends upon the DPOAE phase being rapidly varying, as then the phase contains information about the traveling-wave delay. In the sub-BF region, the reverse wave can be expected as long as the DP amplitude and phase behavior [in panels (C) and (D), (H) and (I)] indicates that the DP is not dominated by local distortion. Except for in these two regions, a reverse wave cannot be expected to be detected (animal wg81).

DPOAE data are plotted as a dotted line in panels (D), (E), (I), and (J). This curve is included to show the forward-traveling-wave phase.

1. Sub-BF region

The BF of both animals in Figs. 7–10 was 21 kHz. At frequencies below ~15 kHz amplitude and phase fine structure was apparent in the DP as well as the DPOAE. The DP phase was not similar to the single-tone response, and the tuning of the DP was not like the single tone (confirming results from Fig. 5) so the DP did not appear to be forward traveling. In some cases details of fine structure in the DP were precisely echoed in the DPOAE (prominent cases are marked with double arrows in Fig. 9) but the general finding is that the sub-BF region of the DP possessed fine structure. Middle ear transmission imposes fine structure on the DPOAE (Dong and Olson, 2006) so we cannot expect every detail in the sub-BF DP to be evident in the DPOAE. The DP fine structure is likely produced by summing interference, either between locally or basally generated and apically generated distortion, or simply between wave-fixed and place-fixed distortion components, both arriving at the basal measurement location from more apical locations. The DPOAEs and DPs exhibited similar level dependence; in Fig. 8, when the stimulus level increased from 60 to 70 dB there was less than a 10 dB change in the response, but the increase to 80 dB caused a greater than 10 dB change in both the DP and DPOAE at most frequencies below 15 kHz [Fig. 8(F) and 8(H)]. The phase of both the DPOAE and DP also changed in character with this level change [Figs. 8(G) and 8(I)]. In the DP the phase slope went from slightly upward sloping to flat and in the DPOAE from flat to slightly downward sloping. In other cases the low-frequency phase of the DP and DPOAE were both relatively rapidly varying, as in panels (B) and (D) of Figs. 7–10 (the $2f_2-f_1$ DP). The rapidly varying DP phase is not similar to the single-tone response and thus does not appear to be locally/basally generated. On the other hand, the large group delay the steep phase represents can be explained as being a reflector emission from more apical locations.

When we plotted the phase DPOAE–DP, it was very similar to the forward-traveling-wave phase in the sub-BF region panels (E) and (J) of Figs. 7–10, which is as expected for a reverse-traveling wave. However, the phase variation was small in this region and not significantly different from what middle-ear transmission delay would produce. Nevertheless, the strong similarity between the forward and reverse phases measured in the same experimental preparation demonstrates a compelling similarity between sound traveling in and sound traveling out of the cochlea.

2. BF region

As we and others have noted (Robles *et al.*, 1997; Dong and Olson, 2005b, a; Olson and Dong, 2006), in a broad region of the BF, the intracochlear DP is usually tuned like a single tone, with a forward-traveling-wave phase. This characteristic is expected for locally generated distortion or a basally generated DP traveling forward. It was also seen in

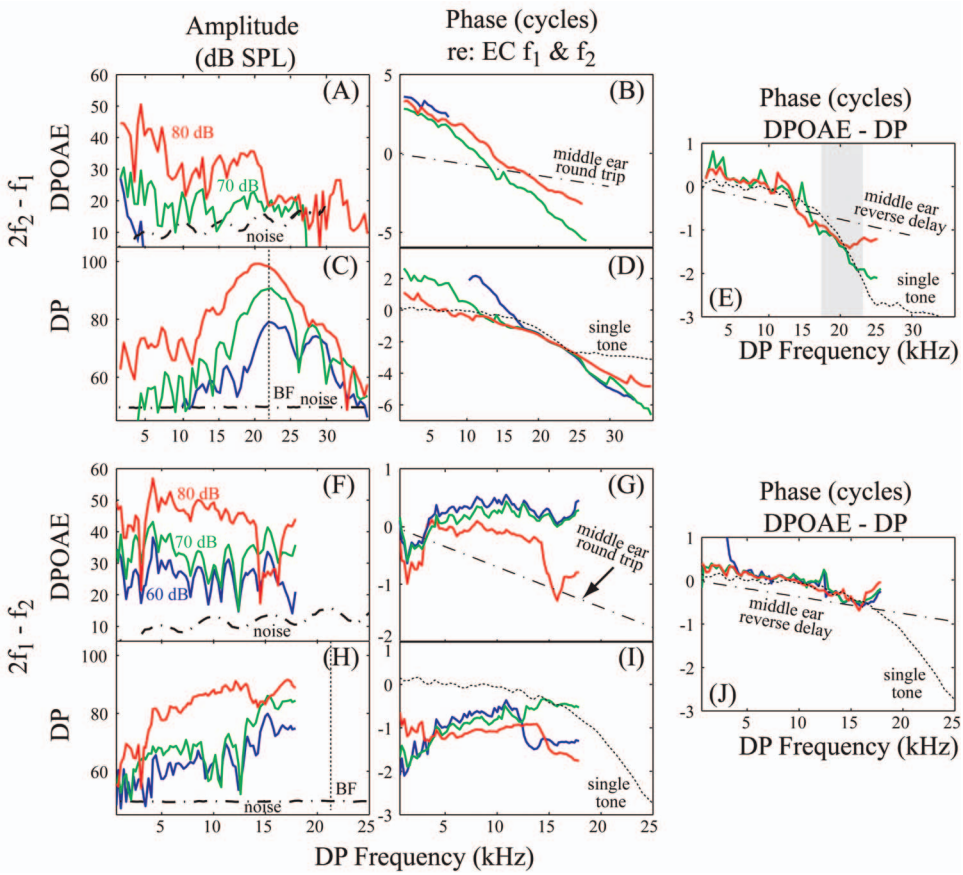

FIG. 8. Simultaneous recording of the DP and DPOAE with $f_2:f_1=1.25$ with the same format, measurement position, and animal as in Fig. 7. In the relative phase data of panel (E), in the BF region [gray bar in panel (E)] the reverse wave was apparent in the 70 dB data (~18–23 kHz region) but less so at the higher, 80 dB SPL level. At the higher level, the DPOAE phase was slightly less steep than at the 70 dB level in the 20–25 kHz region. The $2f_1-f_2$ DP was not recorded in the BF region for this ratio=1.25 case.

the data of Figs. 7–10. Therefore, unlike the sub-BF region, we have no reason to expect that in general the locally measured DP at frequencies around the BF will be responsible for the DPOAE. When we reference the DPOAE phase to the DP, the results take several different shapes.

Starting with Fig. 7(E), the DPOAE–DP phase, after a wiggle at 13–15 kHz, was similar to the forward single-tone phase through and slightly above 20 kHz. The basis for the reverse-wave phase behavior in the BF region can be found in the DPOAE phase, which underwent a change in slope from shallow to steep at ~15 kHz. Comparing the DPOAE and DP phases in the BF region in Fig. 7(E), the DPOAE phase slope was approximately two times the DP phase slope, and the DP phase was forward traveling in character. Therefore it is little wonder that when comparing these phases directly (DPOAE–DP), a reverse wave is indicated. Based on this phase behavior, the DP does appear to be responsible for the DPOAE.

In Fig. 7(J), the $2f_1-f_2$ DPOAE–DP phase was like the single-tone phase in the 20 kHz region. As above, the reason for the similarity is in the DPOAE phase of 7(G), which became steep in the ~18–22 kHz region, with a slope that was approximately twice the forward-traveling DP phase of Fig. 7(I). In Fig. 8(E), the DPOAE–DP phase was similar to the single-tone phase, but only at frequencies very close to the BF. The DPOAE at the 80 dB SPL stimulus level was offset by a full cycle from the 70 dB SPL DPOAE over most of the frequency range, so these two phases are actually approximately equal, although they appear different in the plot. Above 20 kHz, they do diverge slightly, with the 80 dB phase data flattening out somewhat. The 70 dB DPOAE–DP phase was similar to the single-tone data up to ~22 kHz, but with the 80 dB stimulus level the correspondence was more limited.

Data from another animal, in Figs. 9 and 10, showed similar trends. In Figs. 9(E) and 9(J) (60 and 70 dB data), and 10(E) (70 dB data) in the BF region the DPOAE–DP phase was similar to the single-tone phase. In all these cases, the DP was forward traveling, and the DPOAE was steep, with a slope in the BF region approximately equal to twice the forward-traveling phase. However, we see something unexpected in Figs. 9(G), 9(I), and 9(J). The $2f_1-f_2$ DPOAE–DP phase, 80 dB data, in Fig. 9(J) sloped upward with frequency: the DPOAE phase led the DP phase, *as if the DPOAE preceded the DP*. This seemingly paradoxical result is similar to the previously reported finding in which, based on their relative phases, the DP in stapes vibration appeared to precede the intracochlear DP in BM motion (Ren, 2004). The explanation offered in that study was that the DP exited the cochlea essentially instantaneously as a compression (sound) wave, and set the stapes in vibration, which then launched a forward-going traveling wave. On the other hand, the paradox can be adequately explained without invoking an instantaneous compression pressure by revisiting the DPOAE and DP results. At frequencies greater than 15 kHz, the DP phase was that of a forward-going traveling wave [Fig. 9(I)]. This is readily understood as locally generated distortion by the forward-traveling primaries, or basally generated distortion traveling forward. Within the BF frequency region the DPOAE phase had a nearly flat phase [Fig. 9(G)].

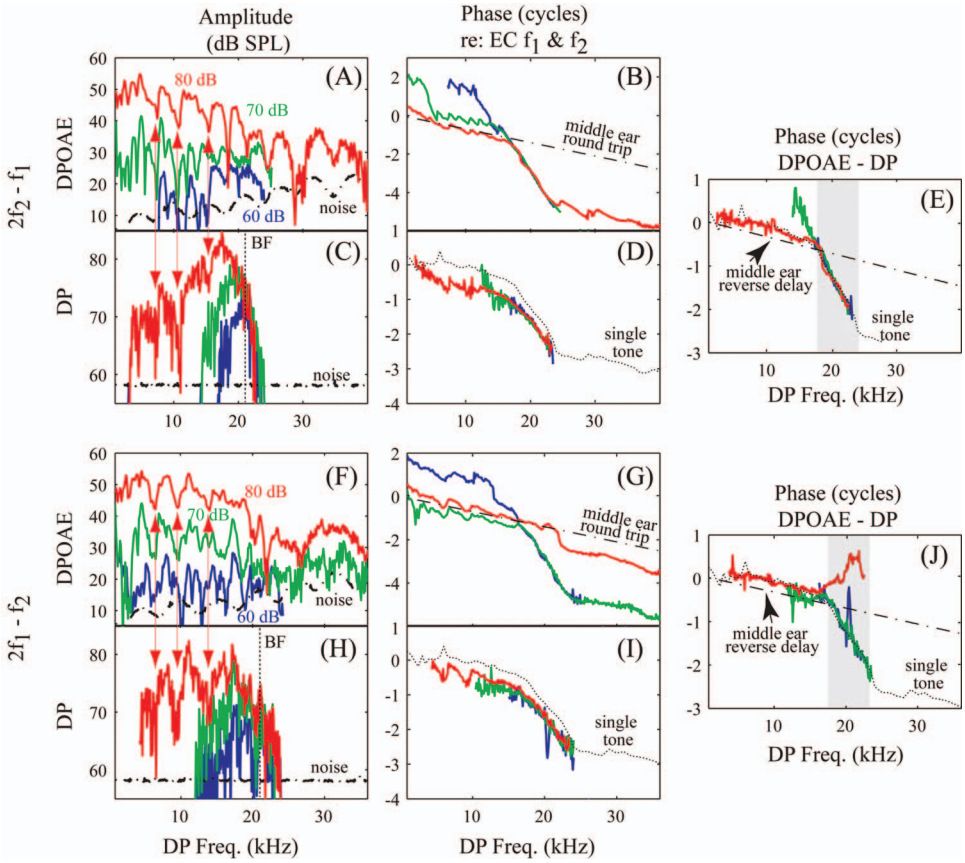

FIG. 9. Simultaneous recording of the DP and DPOAE with f_2:f_1=1.05. L_1 =L_2=60 (blue), 70 (green), and 80 dB SPL (red), sensor positioned 10 μm from the BM, f_2 swept from 1000 to 40 000 in 100 Hz steps. 60 dB SPL data were averaged 50 times rather than the usual 20 times. In the sub-BF region (less than ~14 kHz), the double arrows indicate that the fine structure in DP amplitude was echoed in the DPOAE. The DPOAE–DP phase supported the reverse wave in all cases in which data were available. In the BF region (gray bars) the reverse-traveling wave was only apparent when the DPOAE phase was rapidly varying. When the DPOAE phase was not rapidly varying [panel (G)] (80 dB) relating the DPOAE and DP phases caused a paradoxical result [panel (J)] in which the DPOAE appeared to lead the DP at frequencies close to BF (animal wg96).

This DPOAE phase can also be interpreted within the theory of cochlear emissions, as a wave-fixed/generator emission (Kemp, 1986). However, in a wave-fixed type emission, the slope of the phase-frequency curve is not related to delay. Since the DPOAE and DP phases can be understood individually within the framework of forward and reverse cochlear traveling waves, their relative phase, the DPOAE–DP phase, is therefore also in keeping with that framework, and *is not* at odds with it.

We performed similar measurements with a fixed f_2 stimulus paradigm, and Fig. 11 shows the simultaneous recordings of the $2f_1-f_2$ DP and DPOAE from animal wg96 (the same as in Figs. 9 and 10). With this paradigm the position of the f_2 response pattern was fixed and the overlapping region of f_1 and f_2 response patterns decreased as the f_1 frequency swept from high to low (increasing the f_2:f_1 ratio). Both the DPOAE and the DP were ratio dependent. The amplitude of the DP was ~80 dB from 11 to 19 kHz (11 kHz corresponding to f_2:f_1=1.29), and then decreased quickly with increasing f_2:f_1 ratio. On the other hand, the DPOAE increased slightly as the ratio increased from 1.05 and peaked at 14 kHz [Fig. 11(A)], corresponding to an f_2:f_1 ratio of 1.18. Similar to the DP, the DPOAE also decreased quickly below 11 kHz, corresponding to a f_2:f_1 ratio greater than 1.29 [Fig. 11(A)]. Above 15 kHz, the DP phase-frequency slope was similar to that of the single-tone forward-traveling-wave phase, but below 15 kHz the phase slope was greater than that of the forward-traveling-wave phase. This suggests that at frequencies around the BF, the DP was locally/basally generated, while at sub-BF frequencies it was not. The DPOAE phase was steeper than the DP at frequencies below 15 kHz, but then became shallower. [Unlike the fixed f_2:f_1 ratio paradigm, with the fixed f_2 paradigm the steeply varying DPOAE phase is not a clear indicator of place-fixed emission type, as even a wave-fixed emission is expected to have substantial phase-frequency slope (Shera *et al.*, 2000), so this useful analysis cue is missing in these data.] When we compared DPOAE to DP phases [Fig. 11(C)], the results were similar to those with a fixed ratio. In the sub-BF region, the DPOAE–DP phase overlaid the forward-traveling-wave phase, supporting the reverse-traveling-wave hypothesis. At 15–17 kHz (the region in which the DPOAE phase flattened somewhat) the DPOAE–DP phase sloped upward, as though the DPOAE led the DP, which seems counter to the reverse wave hypothesis (Ren, 2004). In summary, the fixed f_2 DPOAE–DP phase results were similar to the fixed f_2:f_1 ratio results, and showed both reverse-wave and paradoxical behavior. The interpretation of the fixed-ratio-result of Figs. 7–10 benefitted from the ease of separation into wave-fixed/generator and place-fixed/reflector type emissions. These interpretative cues are missing with the fixed f_2 paradigm, but the data are consistent with the same interpretation as in the fixed-ratio case.

3. Grouped data: DPOAE and DP

The exploration for evidence of a reverse wave relied on analysis of the phase responses of the DPOAE and DP. Above, these two responses were compared in individual animals and certain patterns emerged. In particular, in the BF region the reverse wave was only detectable when the

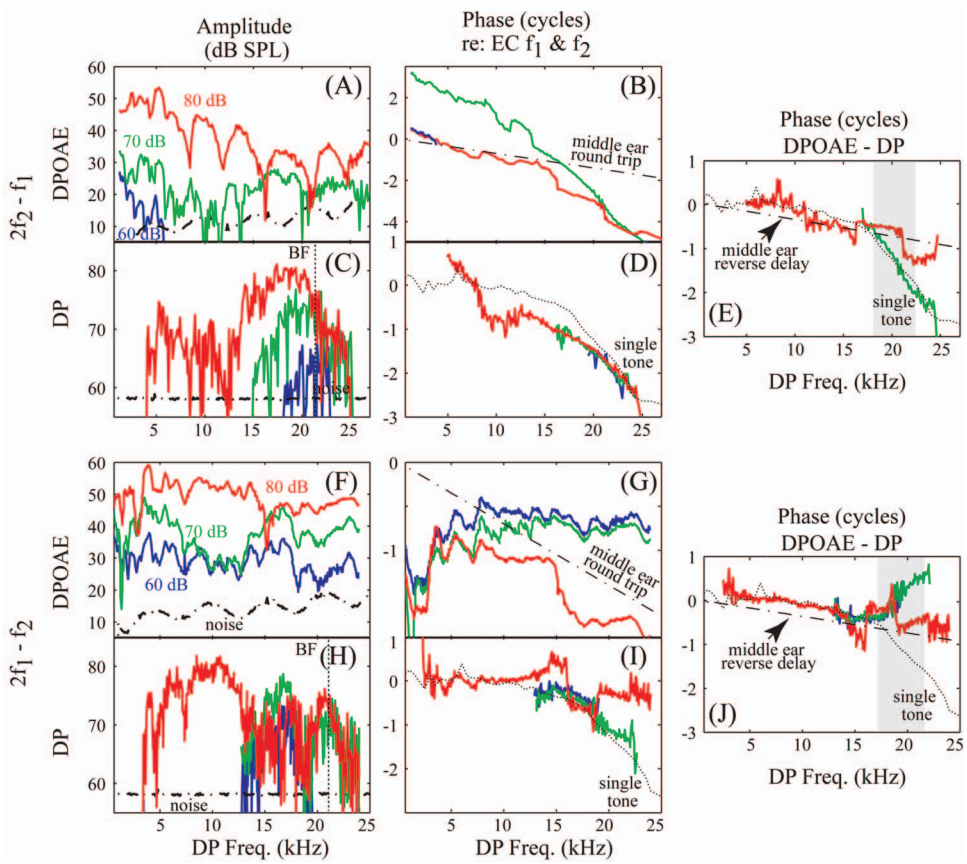

FIG. 10. Simultaneous recording of the DP and DPOAE with $f2:f1=1.25$ with the same format, measurement position, and animal as in Fig. 9. In the BF region (gray bars), the detection of the reverse-traveling wave depends upon the DPOAE phase, which is level dependent. In the BF region (gray bars) the reverse-traveling wave was only apparent when the DPOAE phase was rapidly varying [70 dB stimulus level of panel (B)]. When the DPOAE phase was not rapidly varying [panels (G) and (J)] relating the DPOAE and DP phases caused a paradoxical result in which the DPOAE appeared to lead the DP at frequencies close to BF. In the BF region, the 80 dB stimulus level data in panel (B) are subject to a stair–steplike behavior (coupled to sharp fine structure in the amplitude) that gives rise to a messy DPOAE–DP result.

DPOAE had a rapidly varying phase-frequency response. In order to convey the generality of the DPOAE phase results, in Fig. 12 we show grouped DPOAE data from the eight animals in this study for which the 70 dB stimulus gave emission responses above the noise floor over a relatively wide frequency region. These are more interesting than the 80 dB DPOAEs since they are more apt to show the steep phase-frequency slope of the reflector/place-fixed emission type, whereas the 80 dB DPOAEs tend to show the flat phase-frequency slope of the generator/wave-fixed emission (see DPOAE phase level dependence in Fig. 2). Recall that the group delay of the place-fixed/reflector emission type is related to the group delay of the forward-traveling wave at its BF. If the reverse wave exists, the group delay is expected to be approximately two times the forward-traveling wave group delay at its BF, and if it does not exist, it is expected to be approximately equal to the forward group delay. In order to aid in the comparison, we include a single-tone 50 dB phase-frequency curve from one animal (wg81), multiplied by 2. (The intracochlear location of measurement of all the animals in this study was ~20 kHz, so it is sufficient to include the comparison curve from a single animal.) In contrast to the rapidly varying place-fixed emission phase, the flat phase of the wave-fixed/generator emission, while powerful in its relation to scaling symmetry, does not contain information about forward and reverse group delays (Kemp, 1986; Zweig and Shera, 1995; Shera and Guinan, 1999). Theoretically, the wave-fixed/generator emission is flat

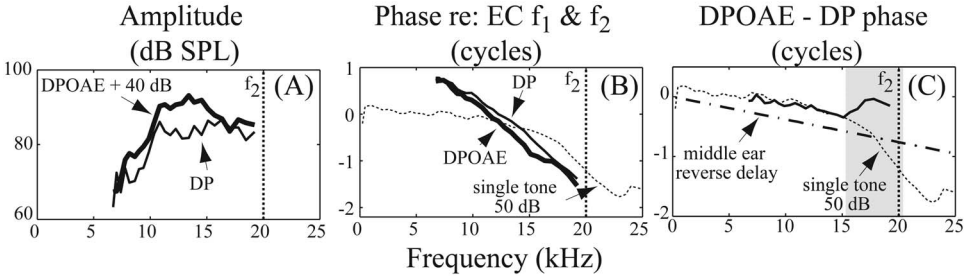

FIG. 11. Simultaneous recordings of $2f_1-f_2$ DP and DPOAE with f_2 fixed at BF. $L_1=L_2=80$ dB SPL, $f_2:f_1$ changed from 1.02 to 1.5 in steps of 0.02. The sensor was positioned 10 μm from the BM. (A) The $2f_1-f_2$ DPOAE (thick line) and DP (thin line) amplitude. The DPOAE amplitude was moved up 40 dB to facilitate the comparison. The vertical line indicates the BF=f_2 frequency. (B) The $2f_1-f_2$ DPOAE (thick) and DP (thin) phase, referenced to EC f_1 and f_2. (C) Phase of DPOAE–DP. The dotted lines show single-tone 50 dB stimulus level response phase relative to the pressure stimulus in the EC. Dotted–dashed lines show average middle-ear reverse delay. The reverse wave was detected in the sub-BF region below 15 kHz (C). Above 15 kHz the DPOAE seemed to lead the DP. Because the stimulus paradigm was not a fixed ratio, the DPOAE phase does not allow for identification of wave-fixed and place-fixed emission type, making interpretation of these data less straightforward than with the fixed-ratio paradigm (animal wg96).

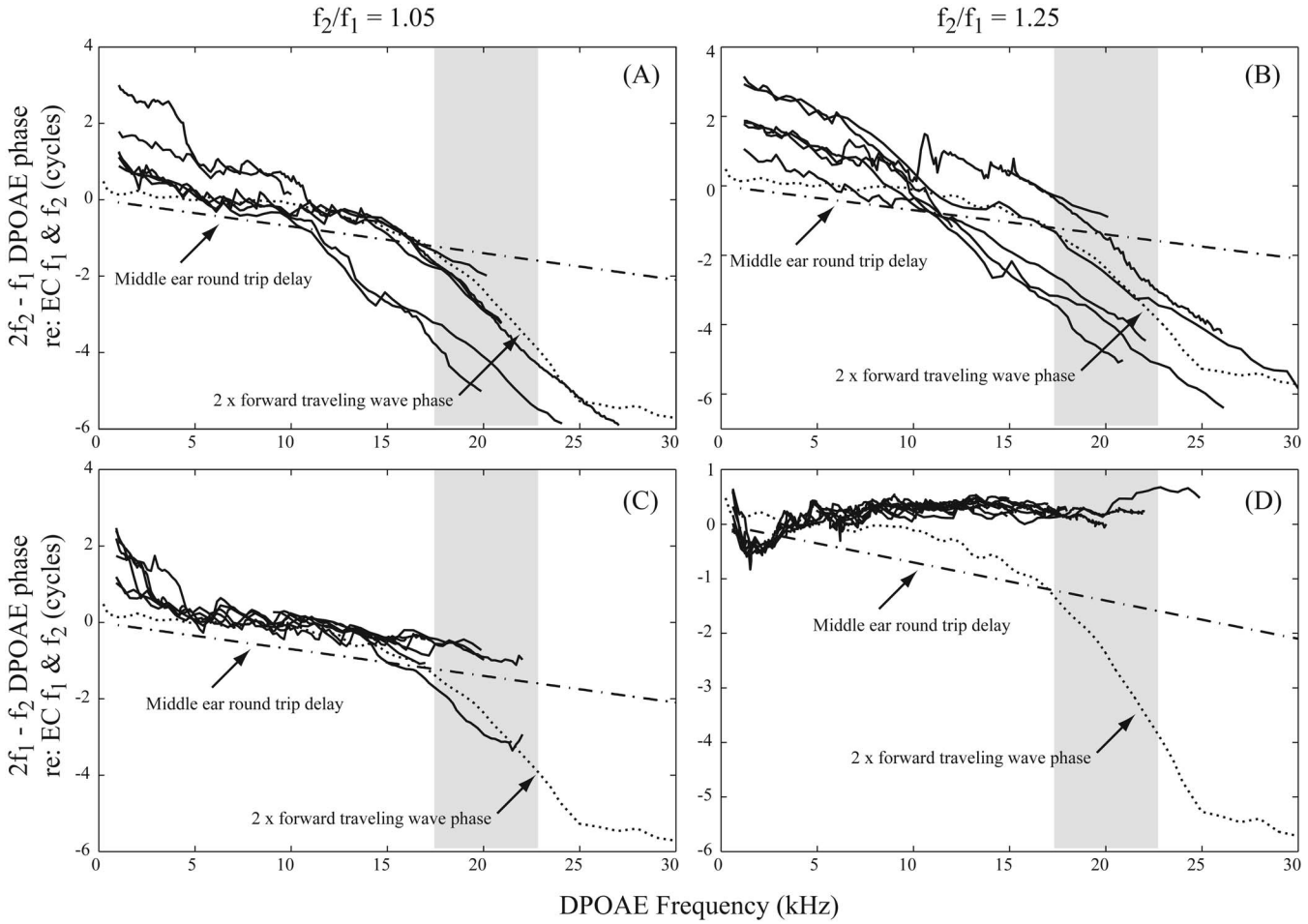

FIG. 12. The grouped phases of the $2f_2-f_1$ and $2f_1-f_2$ DPOAEs from eight animals illustrate the generality of the responses. These preparations had robust DPOAE responses over a wide frequency range for 70 dB primaries. (When the primaries are at a level of 80 dB SPL, the phases tend to flatten, and are less interesting.) All phases were referenced to EC f_1 and f_2 phases. (A) and (B) The $2f_2-f_1$ phase with $f_2:f_1$ ratios of 1.05 and 1.25, respectively. (C) and (D) The $2f_1-f_2$ phase with $f_2:f_1$ ratios of 1.05 and 1.25, respectively. The dotted line is twice the single-tone pressure response phase measured close to the BM from a representative case (wg81, 50 dB SPL), shown for comparison. The dotted–dashed line also shows the average middle-ear round-trip delay for comparison. Gray bars identify the 20 kHz region that can be compared to the DP data gathered during this study, for which the BF was ~20 kHz (animals wg81, wg89, wg90, wg92, wg93, wg94, wg95 and wg96).

within the cochlea, and when measured in the EC would evince middle-ear forward and reverse delays. Therefore, in order to aid the comparison, we also include the average middle-ear round-trip delay phase.

Immediately apparent in Fig. 12 is that the character of each DPOAE type is conserved among animals. The $2f_1-f_2$, 1.05 $f_2:f_1$ ratio DPOAE phase [Fig. 12(C)] was slightly downward sloping at frequencies below 15 kHz, with a slope almost identical to the middle-ear round-trip delay [see also Figs. 2(G), 4(G), 7(G), and 9(G)]. Therefore, within the cochlea this phase would be flat, consistent with a wave-fixed emission. Wiggles appear in the phase data of panel 12(C), suggesting the presence of a lesser contribution from a place-fixed/reflector emission component. The 1.25 $f_2:f_1$ ratio $2f_1-f_2$ phase in panel 12(D) did not show this middle-ear delay, rather the phase slope tended to be nearly flat, or even upward sloping. This was also seen in Figs. 2(H), 4(H), 8(G), and 10(G). Therefore, within the cochlea the DP phase-frequency curve will slope clearly upward. The $2f_2-f_1$ phase often had a gradual slope that was approximately equal to the round-trip middle-ear delay up to a certain frequency, and then abruptly changed to a steeper slope [Figs. 12(A) and 12(B), also in Figs. 2(E) and 2(F), 4(E) and 4(F), 7(B), 8(B), 9(B), and 10(B)]. The underlying cochlear mechanism for the shift point is unknown. We observed in previous figures that the shift generally occurred at lower frequencies for lower stimulus levels [Figs. 2(E) and 2(F), 7(B) and 9(B) and 9(G)]. Theoretically, the steep slope phase corresponds to the place-fixed/reflector emission type. In the ~20 kHz region, the steep slope is similar to twice the forward-traveling-wave delay found in our intracochlear measurements, with BF of ~20 kHz. This is consistent with the presence of a reverse-traveling wave from the 20 kHz region giving rise to the 20 kHz DPOAE. To quantify this correspondence, we found the group delay (negative slope) of the phase-frequency curves at 20 kHz for all the curves in Fig. 12 whose slope was significantly steeper than the middle-ear round-trip delay in the 20 kHz region. This was all of the curves in panels 12(A) and 12(B). The group delays averaged 0.41 ms, with a standard deviation of 0.11 ms. This can be compared with the forward-traveling-wave data (dotted line), whose group delay at 20 kHz was 0.23 ms. When multiplied by 2, as in

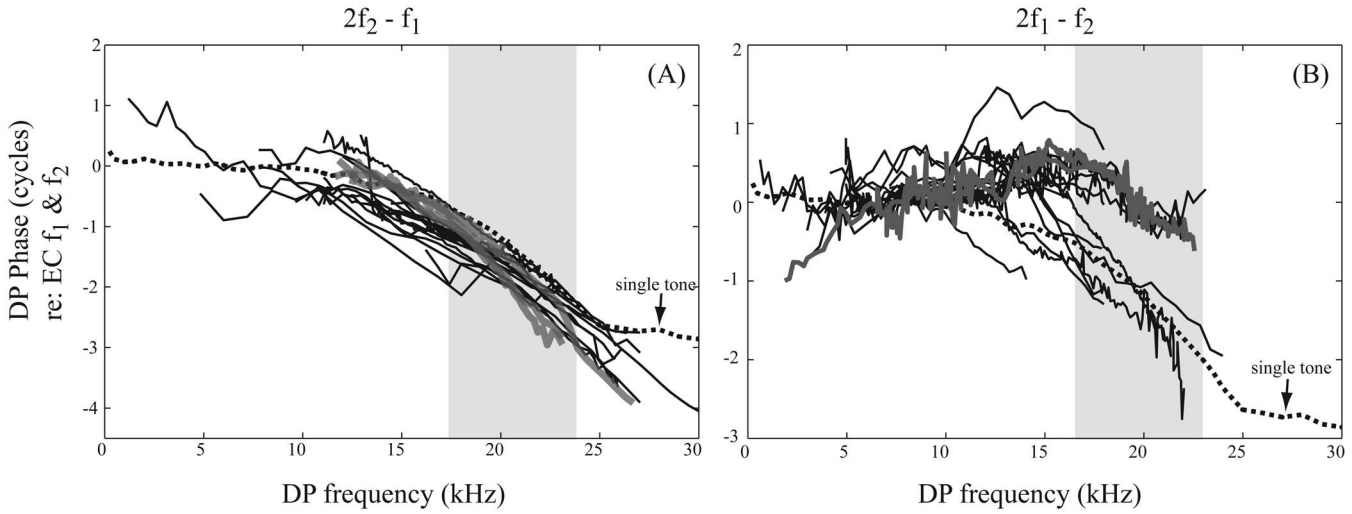

FIG. 13. The $2f_2-f_1$ and $2f_1-f_2$ DP phases from all 17 animals that contributed to this study. The sensor was positioned within 30 μm of the BM, $L_1=L_2=70$ (gray) and 80 dB SPL (black), $f_2:f_1=1.25$. (A) The $2f_2-f_1$ phase; (B) $2f_1-f_2$ phase. All phases referenced to EC f_1 and f_2 phases. The dotted line shows the single-tone response phase measured close to the BM from a representative case (wg81, 50 dB SPL), shown for comparison. The $2f_2-f_1$ phases overlaid the single-tone (forward-traveling wave) phase at frequencies in a broad BF region, indicating that local distortion dominated the DP there. The $2f_1-f_2$ DP phase sloped up at low frequencies, and was not similar to the single-tone response there. In the region of the BF, the phase typically sloped downward similarly to the single-tone phase, suggesting a forward-traveling-wave DP in this frequency region. The gray bar identifies the ~20 kHz BF region probed in this study.

the figure, this is 0.46 ms. Scatter is expected; the reflector emission is not expected to emerge from a point in the cochlea, but rather from the region within the cochlea where the DP is relatively large (Shera and Guinan, 2003).

Figure 13 shows grouped DP phase data from all the animals used in this study. The stimulus level of the plotted curves was in general 80 dB SPL (black curves), but several results found with a stimulus level of 70 dB SPL curves are included (gray curves) and show that those results are similar. (Also see Figs. 5 and 7–10, which show that level does not change the DP phase significantly in the BF region.) The 80 dB data are emphasized in Fig. 13 in order to include all the study animals in the plot with results above the noise through a wide frequency region, and the similarity with 70 dB data when they are available justifies this emphasis. With the 1.25 $f_2:f_1$ ratio, the $2f_1-f_2$ and $2f_2-f_1$ results were quite different from one another. [The 1.05 $f_2:f_1$ ratio DPs both look similar to each other, and were similar to the $2f_2-f_1$ results at the 1.25 $f_2:f_1$ ratio, and are not shown. Extensive observations on the 1.05 ratio DP were presented previously (Dong and Olson, 2005b, a; Olson and Dong, 2006).] Like the DPOAE, the character of the different DPs is conserved among animals. Throughout the broad BF region, the $2f_2-f_1$ DP phase has the forward-traveling-wave character that is easily attributable to local or basally generated distortion. At frequencies somewhat below the BF (below ~15 kHz), this similarity breaks down, signaling a lack of dominantly local distortion. These characteristics confirm the generality of the $2f_2-f_1$ results highlighted in Figs. 7 and 9. The $2f_1-f_2$ DP sloped mildly upward up to ~15 kHz. Close to the 20 kHz BF, the slope was usually downward, with a slope similar to the single-tone phase, which would occur if the DP had traveled to the BF location postgeneration. These characteristics of the grouped data confirm the generality of the $2f_1-f_2$ results in Figs. 5, 8, and 10.

IV. DISCUSSION

DPOAEs are a noninvasive measure of cochlear mechanics. The single place measurement of the DPOAE reflects processes that occurred within the cochlea's complex three-dimensional (3D) structure. The use of the DPOAE to probe these processes has proceeded with certain simplifying assumptions. A robust feature of cochlear mechanics is a forward-traveling wave, and one of the assumptions built into theories of emissions was that they proceed out of the cochlea as a reverse-traveling wave. Many characteristics of DPOAEs do support the reverse-wave picture. However, a recent study aimed at detecting the reverse wave within the cochlea did not detect it (Ren, 2004; He *et al.*, 2007). Those experiments worked as follows: a 1 mm extent of BM was examined. BM velocity was measured. Two-tone stimulation was applied, and the response measured and analyzed to reveal the spatiotemporal pattern of f_1, f_2 and $2f_1-f_2$. Responses at f_1 and f_2 frequencies were observed to travel forward: their phase lags accumulated with distance from the stapes. A wave traveling in the other direction—out of the cochlea, would accumulate phase lag as it got closer to the stapes. When the $2f_1-f_2$ intracochlear DP was examined, it also accumulated phase lag with distance from stapes, indicating a forward-traveling wave. Following up, intracochlear DPs in BM motion were compared with stapes DPs (a proxy for the DPOAE). A fixed f_2, swept f_1 paradigm was used, with f_2 either close to or ~1/2 octave below the local BF. The phase-frequency slope of the BM DP was compared to the DP on the stapes. The BM DP had the steeper slope (indicating greater delay), suggesting that the stapes DP preceded the BM DP. Faced with these observations, an alternative process to the reverse wave was hypothesized, in which

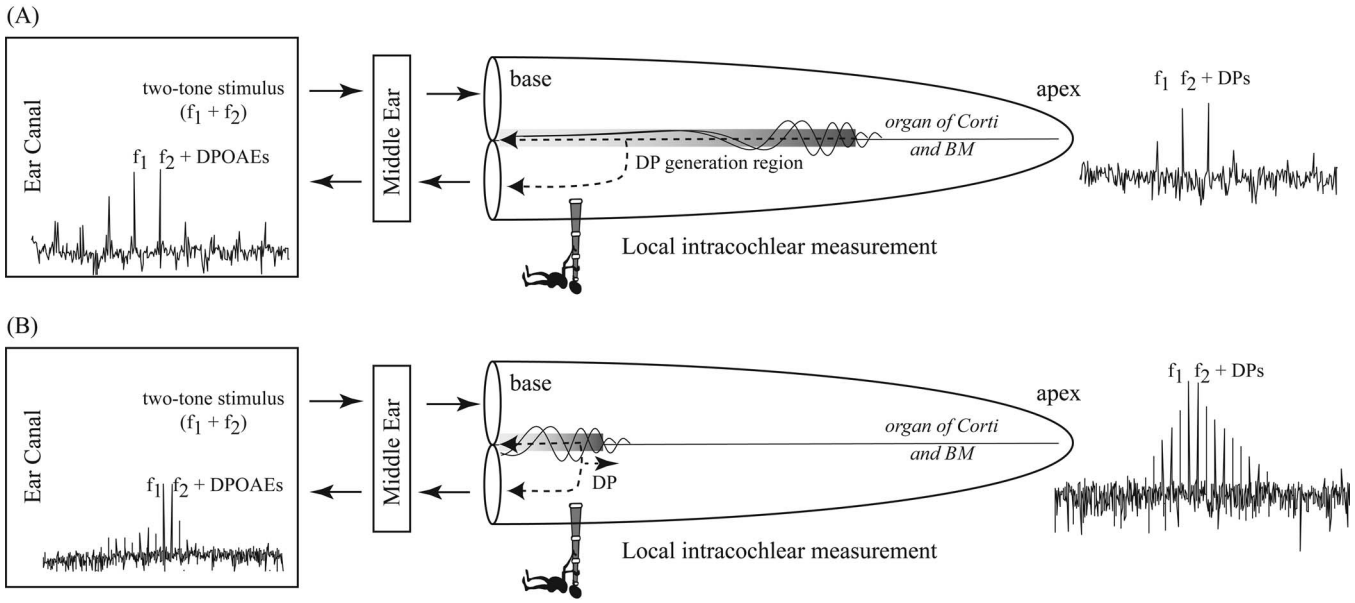

FIG. 14. Illustration of the generation and transmission of DPs. Upon two-tone stimulation, distortion products are generated by cochlear nonlinearity and can be detected within the cochlea as DPs and in the ear canal as DPOAEs. The pressure sensor was positioned at the basal turn of the cochlea where the BF was ~20 kHz. In (A) the primary f_1 and f_2 frequencies were well beneath the local BF. In this case the sub-BF DP is likely generated apical of our sensor location, and when detected, is on its way out of the cochlea. In (B) the primary f_1 and f_2 frequencies are in the BF region. In this case the DP was generated close to our sensor position, and is relatively large due to cochlear tuning of both the primaries and the DP. It has a forward-going character due to the forward-going character of the primaries.

DPs are transported out of the cochlea as a compression wave, where they excite the stapes and launch a forward-going wave at the DP frequency.

Many of our results are in accord with those of Ren. In particular, we show that the intracochlear DP has a forward-traveling behavior in a broad frequency region near BF. We also observed a DPOAE phase-frequency slope that was shallower than the DP phase-frequency slope. However, these results are not in disaccord with the reverse-traveling wave. We back up this statement below, starting by reviewing DPOAE and DP results (see also Shera *et al.*, 2005).

A. General characteristics of the DPOAE and DP

In the most general terms, the DPOAE is a complex, broad-frequency-band response. DPOAE amplitude data possessed fine structure: peaks and sharp minimums. The constructive and destructive summing of the two emission types (generator/wave fixed and reflector/place fixed) is thought to give rise to the amplitude fine structure (Stover *et al.*, 1996; Talmadge *et al.*, 2000; Kalluri and Shera, 2001). The DPOAE is diminished at frequencies above 25 kHz. These frequencies are represented in the fragile, basal region of the cochlea, and it is possible that the above-BF frequency rolloff occurred because cochlear nonlinearity had been compromised in this region.

Phase is key to this study. Emissions are known to exhibit two strikingly different phase behaviors (Kemp, 1986; Shera and Guinan, 1999). With fixed $f_2:f_1$ ratio, the DPOAE phase can be almost flat with frequency, or can be rapidly rotating through several cycles. These behaviors correspond, respectively, to the generator/wave-fixed and reflector/place-fixed emission types. It has been observed that the high-frequency-side DPOAEs (e.g., $2f_2-f_1$) are more apt to exhibit the steep phase-frequency slope, whereas the low-frequency-side DPOAEs (e.g., $2f_1-f_2$) tend to exhibit the flat slope (Knight and Kemp, 2000, 2001). It has also been observed that with increases in stimulus level, the DPOAE phase tends to flatten (Mauermann *et al.*, 1999; Mauermann and Kollmeier, 2004). We observed these characteristic DPOAE phase behaviors.

The DP was measured at a single position in the cochlea with BF ~20 kHz. The character of the DP was different for frequencies in the vicinity of the local BF and for frequencies below the local BF. Figure 14 is a cartoon illustration of the cochlear situation for sub-BF DPs [Fig. 14(A)] and approximately BF DPs [Fig. 14(B)], which is useful for understanding the dichotomy. At frequencies in a broad region around the BF the DPs were tuned, in some cases even more sharply than their parent primaries. The DP tuning in evidence supports the idea that even at high stimulus levels a DPOAE would be substantially contributed to by its own BF frequency region of the cochlea. In this frequency region, the phase was forward traveling. This forward-traveling phase is expected, since the DP is produced by the nonlinear response of the forward traveling primaries [Fig. 14(B)]. In addition, after being produced a DP would be expected to travel forward within the cochlea to its own best place (Robles *et al.*, 1997; Dong and Olson, 2005b).

At frequencies below the BF, the DP amplitude showed fine structure that was similar to the behavior of a DPOAE, suggesting that the DPs had been contributed to by more than one component. The wide ratio of 1.25 $2f_1-f_2$ results often showed a pronounced bimodal shape separated by a sharp minimum, as in Figs. 3(D), 5(B) and 10(H). The presence of this apparent interference notch also supports a dual

or multicomponent picture of the DP. In the sub-BF region, the phase departed from the forward-traveling-wave pattern, consistent with apical DP generation. It is reasonable to expect that sub-BF DPs are substantially contributed to by apically generated distortion, traveling through the more basal region of the cochlea to emerge from the cochlea as an emission [Fig. 14(A)]. Therefore the DPs are expected to be on their way out of the cochlea when we measure them. In support of this idea, robust DP nonlinearity does exist throughout the cochlea, including the apex, as illustrated by auditory nerve recordings (Kim and Molnar, 1979) and apical turn mechanics (Khanna and Hao, 1999; Cooper and Dong, 2002; Khanna, 2002; Cooper, 2006).

B. Relating DPs and DPOAEs

The signature of a traveling wave is in the phase response, and the signature of a reverse-cochlear traveling wave will lie in a DPOAE–DP phase that is similar to the well established single-tone response phase. This study was aimed at this result. We found that this pure result, the DPOAE–DP phase alone, was not definitive, but that by considering this phase in conjunction with the DP and DPOAE results, more compelling conclusions could be drawn.

1. At frequencies below BF

At substantially sub-BF stimulation frequencies, based on both amplitude and phase, DPs appeared to be generated apical of our basal measurement location. Therefore the DPs are expected to be on their way out of the cochlea when we measure them and it is reasonable to look for a reverse-wave characteristic in the DPOAE–DP phase. Note that it is the behavior of the DP that forms the basis for this reasonableness, and it applies regardless of the character of the DPOAE. If the measured DP travels out of the cochlea as a traveling wave then the phase, DPOAE–DP, will overlie the forward-traveling-wave phase. If on the other hand, the DP travels out of the cochlea instantaneously as a compressive pressure, the DPOAE–DP phase will overlie the reverse middle-ear phase. When their phases were related (DPOAE–DP), the phase-frequency relationship was similar to the forward-traveling-wave phase. However, in this sub-BF region, the forward-traveling-wave phase does not change rapidly, and therefore the DPOAE–DP phase does not demonstrate clear reverse-traveling-wave phase behavior. The strong similarity between single-tone transmission into the cochlea and DP transmission out of the cochlea as a traveling wave was nevertheless striking. This striking similarity, coupled with the qualitative similarity between the DP and the DPOAE, and the *lack of similarity* between the DP and the single-tone response in the low-frequency region, does lead to a parsimonious conclusion that these low-frequency DPs were passing through the basal region of the cochlea to give rise to the DPOAE.

2. At frequencies around BF

At frequencies around BF, the DP essentially always showed a forward-traveling-wave phase, and therefore our criterion above for "reasonable reverse-wave case" was never satisfied. However, the steeply phase-sloped "reflector/place-fixed" DPOAE is expected to reveal forward+reverse group delay from the local BF place. Therefore, the steep-phased DPOAE can be reasonably related to the DP in the region of the BF. Note that here it is the behavior of the DPOAE that forms the basis for this reasonableness. In Figs. 7(B) and 7(G) the DPOAE is steep phased in the BF region, and in the DPOAE–DP phase, a reverse wave is apparent, and similarly for Figs. 8(B), 9(B), and 9(G), and 10(B). The grouped data of Fig. 12 confirmed that the phase-frequency slope at 20 kHz of the place-fixed DPOAE, is roughly twice the phase-frequency slope of the forward-going wave, at its 20 kHz BF.

In Figs. 8(G) and 10(G), the high ratio 1.25 $2f_1-f_2$ case, the DPOAE never became steep phased, so the criterion for a "reasonable case" was never met. If we look for a reverse wave in the BF region by plotting the DPOAE–DP phase when the DPOAE was flat phased or had only a mild (middle-ear round-trip) phase slope, the results were like those in Fig. 8(J) at frequencies greater than 17 kHz, in Fig. 9(J) greater than 17 kHz (80 dB stimulus levels), and in Fig. 10(J). In these cases, the DPOAE–DP phase sloped upward, with almost a mirror image of the forward-traveling-wave phase, as though the DPOAE preceded the DP. A similar observation was one of the bases for the hypothesis that the DP traveled out of the cochlea as a compression wave (Ren, 2004). In light of the forward-traveling wave DP, and the flat-phased DPOAE, Ren interpreted this upward slope of the DPOAE–DP phase to mean that the DPOAE must have occurred before the DP. However, here we show that this upward slope is exactly what is to be expected for a forward-traveling-wave DP and a flat-phased DPOAE produced by scaling symmetry.

C. DP spatial variation

In Sec. IV B 2, we show and attempt to understand paradoxical results at frequencies around the BF in which, when a DP was related to a DPOAE via the phase of the two responses, the DPOAE appeared to precede the DP that is expected to be its precursor. We further showed that by looking at the DPOAE–DP phase in specific interpretable frequency regions, a reverse wave was in evidence. However, given the obvious pitfalls in relating phase responses, it is useful to be able to explore the question of reverse-traveling waves from a completely different vantage point. Spatial pressure variations provide this.

As introduced in Figs. 1(B) and 1(C), the intracochlear response to sound comprises two modes: the traveling-wave and compression wave. Theoretically, the pressure distributions of these two pressure modes within the cochlea are strikingly different. At frequencies in the region of the BF, the traveling-wave pressure, being governed by BM width and traveling-wave wavelength, is expected to vary over distances of tens of micrometers (Steele and Taber, 1979b; Andoh and Wada, 2004; Yoon *et al.*, 2006). At the same frequencies the compression pressure will vary over distances corresponding to quarter sound wavelengths—centimeters (Peterson and Bogert, 1950). The compression pressure can

be thought of as a time varying, approximately space filling pressure. Experimentally, these two pressure modes have been detected in the spatial variation of pressure with single-tone stimulation, where it was found that the slow traveling wave dominated close to the BM, ~100 μm from it the compression pressure dominated, producing a spatially invariant pressure (Olson, 1998, 1999, 2001; Dong and Olson, 2005b) in amplitude and phase. Therefore, a marked advantage of pressure measurements is that they can detect both the compression and slow-traveling-wave pressure modes. It has been proposed that DPs travel from their place of generation to the stapes through the cochlear fluid as a compression pressure, another possibility is that they are transmitted via a reverse cochlear traveling wave. The spatial pressure variation of the DPs is a criterion to distinguish the two possibilities: a rapid spatial variation argues for the reverse-traveling-wave mode, whereas if the DP pressure is spatially unvarying, the compression mode is supported. The results in Fig. 6 and results in Dong and Olson (2005b) showed that the DP pressure dropped sharply with distance from the BM. Therefore, the DP pressure distribution within the cochlea appears to be dominated by the traveling-wave pressure mode.

Given the observation that the DP pressure falls into the noise with distance from the BM, the DP compression pressure plateau, if one exists, must be less than 60 dB SPL in the cochlea (the sensor noise floor). Therefore, with the 40 dB loss from the middle-ear reverse transmission (Dong and Olson, 2006), the contribution to the DPOAE from the compression mode would be at most 20 dB SPL, which is much lower than the actual DPOAE we have measured in the EC. In summary, the spatial variation measurement does not rule out a contribution by a compression wave to the DPOAE, but does set the maximum limit of its contribution to DPOAE. Our results suggest that the reverse-traveling wave plays the more important role in DP reverse transmission.

V. SUMMARY

(1) Regarding intracochlear distortion: at frequencies in the broad vicinity of the BF, the DPs were tuned similarly to the primaries, with primarylike forward-traveling phase. This is consistent with distortion that was either generated locally or generated basally and carried to the measurement point by a DP traveling wave. At frequencies substantially lower than the local BF, the DPs did not behave like the primaries, and did not have the forward-traveling-wave phase of the primaries. They instead behaved more like a DPOAE.

(2) Regarding relating DPOAEs to DPs to attempt to observe the reverse wave directly, this can sometimes be done at sub-BF frequencies, for which the DP was not dominated by a forward-traveling DP. In these cases, the DPOAE–DP phase overlaid the forward phase of a primary response, consistent with a reverse cochlear traveling wave. The sub-BF region corresponds to a region of little phase variation, so does not amount to a compelling detection of reverse-traveling wave. Nevertheless, coupled to the similar characters of the DP and the DPOAE and the nonforward-traveling character of the DP, the combined results strongly favor the reverse-traveling-wave description of the sub-BF results. At frequencies in a broad-frequency region of the local BF, the DP was forward traveling. Here, a correlation between the DP and DPOAE can only be reasonably attempted very close to the BF, and only when the DPOAE had a rapidly varying phase. (More concretely, it cannot be attempted when the DPOAE phase was flat or nearly flat, as then the DPOAE phase frequency did not contain cochlear travel-time information.) When the DPOAE did have a rapidly varying phase, the reverse wave was detected, in that the DPOAE–DP phase did closely overlie the primary phase.

(3) The observed spatial dropoff in DP pressure with distance from the DP is inconsistent with a compression pressure DP, but consistent with a traveling-wave DP.

In summary, the data show that DPs are carried along the cochlea by traveling waves and provide compelling evidence against the hypothesis that high level DPs produce compression-pressure waves. The data offer strong supporting evidence for the reverse-traveling wave.

ACKNOWLEDGMENTS

We gratefully acknowledge the efforts of E. de Boer, R. A. Eatock, D. N. Sheppard, C. A. Shera, and two anonymous reviewers, who provided valuable comments on the manuscript. This work was funded by Grant No. R01 DC03130 from the NIH/NIDCD.

NOMENCLATURE

BF = best frequency
BM = basilar membrane
CAP = compound action potential
DP = distortion product
DPOAE = distortion product otoacoustic emission
EC = ear canal
ST = scala tympani
SV = scala vestibuli

Andoh, M., and Wada, H. (**2004**). "Prediction of the characteristics of two types of pressure waves in the cochlea: Theoretical considerations," J. Acoust. Soc. Am. **116**, 417–425.

Avan, P., Bonfils, P., Gilain, L., and Mom, T. (**2003**). "Physiopathological significance of distortion-product otoacoustic emissions at $2f1-f2$ produced by high- versus low-level stimuli," J. Acoust. Soc. Am. **113**, 430–441.

Avan, P., Magnan, P., Smurzynski, J., Probst, R., and Dancer, A. (**1998**). "Direct evidence of cubic difference tone propagation by intracochlear acoustic pressure measurements in the guinea-pig," Eur. J. Neurosci. **10**, 1764–1770.

Cooper, N. P. (**2003**). "Compression in the peripheral auditory system," in *Compression from Cochlear to Cochlear Implants*, edited by S. P. Bacon, R. R. Fay, and A. N. Popper (Springer, New York), pp. 18–61.

Cooper, N. P. (**2006**). "Mechanical preprocessing of amplitude-modulated sounds in the apex of the cochlea," Journal for Oto-Rhino-Laryngology and its Related Specialities **68**, 353–358.

Cooper, N. P., and Dong, W. (**2002**). "Baseline position shifts and mechanical compression in the apical turns of the cochlea," in *Biophysics of the Cochlea from Molecules to Models*, edited by A. W. Gummer, E. Dalhoff,

M. Nowotny, and M. P. Scherer (World Scientific, Titisee, Germany), pp. 261–267.
Cooper, N. P., and Shera, C. A. (**2004**). "Backward traveling waves in the cochlea? Comparing basilar membrane vibrations and otoacoustic emissions from individual guinea-pig ears," in *Proceedings of The Association for Research in Otolaryngology 2004 Midwinter Meeting*, Feb. 22–26, Daytona Beach, Florida.
Decraemer, W. F., de La Rochefoucauld, O., Dong, W., Khanna, S. M., Dirckx, J. J., and Olson, E. S. (**2007**). "Scala vestibuli pressure and three-dimensional stapes velocity measured in direct succession in gerbils," J. Acoust. Soc. Am. **121**, 2774–2791.
Dong, W., and Olson, E. S. (**2005a**). "Tuning and travel of two tone distortion in intracochlear pressure," in *Auditory Mechanisms: Processes and Models, The 9th International Symposium*, edited by A. L. Nuttall, T. Ren, P. Gillespie, K. Grosh, and E. de Boer (World Scientific, Portland, Oregon), pp. 56–62, July 23–28, Oregon.
Dong, W., and Olson, E. S. (**2005b**). "Two-tone distortion in intracochlear pressure," J. Acoust. Soc. Am. **117**, 2999–3015.
Dong, W., and Olson, E. S. (**2006**). "Middle ear forward and reverse transmission in gerbil," J. Neurophysiol. **95**, 2951–2961.
Goldstein, J. L. (**1967**). "Auditory nonlinearity," J. Acoust. Soc. Am. **41**, 676–689.
He, W., Nuttall, A. L., and Ren, T. (**2007**). "Two-tone distortion at different longitudinal locations on the basilar membrane," Hear. Res. **228**, 112–122.
Kalluri, R., and Shera, C. A. (**2001**). "Distortion-product source unmixing: A test of the two-mechanism model for DPOAE generation," J. Acoust. Soc. Am. **109**, 622–637.
Kemp, D. T. (**1978**). "Stimulated acoustic emissions from within the human auditory system," J. Acoust. Soc. Am. **64**, 1386–1391.
Kemp, D. T. (**1986**). "Otoacoustic emissions, travelling waves and cochlear mechanisms," Hear. Res. **22**, 95–104.
Khanna, S. M. (**2002**). "Non-linear response to amplitude-modulated waves in the apical turn of the guinea pig cochlea," Hear. Res. **174**, 107–123.
Khanna, S. M., and Hao, L. F. (**1999**). "Nonlinearity in the apical turn of living guinea pig cochlea," Hear. Res. **135**, 89–104.
Kim, D. O., and Molnar, C. E. (**1979**). "A population study of cochlear nerve fibers: Comparison of spatial distributions of average-rate and phase-locking measures of responses to single tones," J. Neurophysiol. **42**, 16–30.
Kim, D. O., Molnar, C. E., and Matthews, J. W. (**1980**). "Cochlear mechanics: Nonlinear behavior in two-tone responses as reflected in cochlear-nerve-fiber responses and in ear-canal sound pressure," J. Acoust. Soc. Am. **67**, 1704–1721.
Knight, R. D., and Kemp, D. T. (**2000**). "Indications of different distortion product otoacoustic emission mechanisms from a detailed $f1, f2$ area study," J. Acoust. Soc. Am. **107**, 457–473.
Knight, R. D., and Kemp, D. T. (**2001**). "Wave and place fixed DPOAE maps of the human ear," J. Acoust. Soc. Am. **109**, 1513–1525.
Lighthill, M. J. (**1981**). "Energy flow in the cochlea," J. Fluid Mech. **106**, 149–213.
Lukashkin, A. N., Lukashkina, V. A., and Russell, I. J. (**2002**). "One source for distortion product otoacoustic emissions generated by low- and high-level primaries," J. Acoust. Soc. Am. **111**, 2740–2748.
Mauermann, M., and Kollmeier, B. (**2004**). "Distortion product otoacoustic emission (DPOAE) input/output functions and the influence of the second DPOAE source," J. Acoust. Soc. Am. **116**, 2199–2212.
Mauermann, M., Uppenkamp, S., van Hengel, P. W., and Kollmeier, B. (**1999**). "Evidence for the distortion product frequency place as a source of distortion product otoacoustic emission (DPOAE) fine structure in humans. II. Fine structure for different shapes of cochlear hearing loss," J. Acoust. Soc. Am. **106**, 3484–3491.
Mills, D. M. (**2002**). "Interpretation of standard distortion product otoacoustic emission measurements in light of the complete parametric response," J. Acoust. Soc. Am. **112**, 1545–1560.
Olson, E. S. (**1998**). "Observing middle and inner ear mechanics with novel intracochlear pressure sensors," J. Acoust. Soc. Am. **103**, 3445–3463.
Olson, E. S. (**1999**). "Direct measurement of intra-cochlear pressure waves," Nature (London) **402**, 526–529.
Olson, E. S. (**2001**). "Intracochlear pressure measurements related to cochlear tuning," J. Acoust. Soc. Am. **110**, 349–367.
Olson, E. S. (**2004**). "Harmonic distortion in intracochlear pressure and its analysis to explore the cochlear amplifier," J. Acoust. Soc. Am. **115**, 1230–1241.
Olson, E. S., and Dong, W. (**2006**). "Nonlinearity in intracochlear pressure," Journal for Oto-Rhino-Laryngology and Related Specialities **68**, 359–364.
Overstreet, E. H., 3rd, Richter, C. P., Temchin, A. N., Cheatham, M. A., and Ruggero, M. A. (**2003**). 'High-frequency sensitivity of the mature gerbil cochlea and its development," Audiol. Neuro-Otol. **8**, 19–27.
Peterson, L. C., and Bogert, B. P. (**1950**). "A dynamical theory of the cochlea," J. Acoust. Soc. Am. **22**, 369–381.
Ren, T. (**2004**). "Reverse propagation of sound in the gerbil cochlea," Nat. Neurosci. **7**, 333–334.
Robles, L., and Ruggero, M. A. (**2001**). "Mechanics of the mammalian cochlea," Physiol. Rev. **81**, 1305–1352.
Robles, L., Ruggero, M. A., and Rich, N. C. (**1997**). "Two-tone distortion on the basilar membrane of the chinchilla cochlea," J. Neurophysiol. **77**, 2385–2399.
Ruggero, M. A. (**2004**). "Comparison of group delays of $2f1-f2$ distortion product otoacoustic emissions and cochlear travel times," Acoustic Research Letters Online **5**, 143–147.
Ruggero, M. A., and Temchin, A. N. (**2007**). "Similarity of traveling-wave delays in the hearing organs of humans and other tetrapods," J. Assoc. Res. Otolaryngol. **8**, 153–166.
Ryan, A. (**1976**). "Hearing sensitivity of the mongolian gerbil, Meriones unguiculatis," J. Acoust. Soc. Am. **59**, 1222–1226.
Shera, C. A., and Guinan, J. J., Jr. (**1999**). "Evoked otoacoustic emissions arise by two fundamentally different mechanisms: A taxonomy for mammalian OAEs," J. Acoust. Soc. Am. **105**, 782–798.
Shera, C. A., and Guinan, J. J., Jr. (**2003**). "Stimulus-frequency-emission group delay: A test of coherent reflection filtering and a window on cochlear tuning," J. Acoust. Soc. Am. **113**, 2762–2772.
Shera, C. A., Guinan, J. J., Jr., and Oxenham, A. J. (**2002**). "Revised estimates of human cochlear tuning from otoacoustic and behavioral measurements," Proc. Natl. Acad. Sci. U.S.A. **99**, 3318–3323.
Shera, C. A., Talmadge, C. L., and Tubis, A. (**2000**). "Interrelations among distortion-product phase-gradient delays: Their connection to scaling symmetry and its breaking," J. Acoust. Soc. Am. **108**, 2933–2948.
Shera, C. A., Tubis, A., and Talmadge, C. L. (**2005**). "Four counter-arguments for slow-wave OAEs," in *Auditory Mechanisms: Processes and Models, Proceedings of the 9th International Symposium*, edited by A. L. Nuttall, T. Ren, P. Gillespie, K. Grosh, and E. de Boer (World Scientific, Portland, Oregon), pp. 449–457, July 23–28.
Sokolich, W. G. (**1977**). "Improved acoustic system for auditory research," J. Acoust. Soc. Am. **62**, S12.
Steele, C. R., and Taber, L. A. (**1979a**). "Comparison of WKB and finite difference calculations for a two-dimensional cochlear model," J. Acoust. Soc. Am. **65**, 1001–1006.
Steele, C. R., and Taber, L. A. (**1979b**). "Comparison of WKB calculations and experimental results for three-dimensional cochlear models," J. Acoust. Soc. Am. **65**, 1007–1018.
Stover, L. J., Neely, S. T., and Gorga, M. P. (**1996**). "Latency and multiple sources of distortion product otoacoustic emissions," J. Acoust. Soc. Am. **99**, 1016–1024.
Talmadge, C. L., Long, G. R., Tubis, A., and Dhar, S. (**1999**). "Experimental confirmation of the two-source interference model for the fine structure of distortion product otoacoustic emissions," J. Acoust. Soc. Am. **105**, 275–292.
Talmadge, C. L., Tubis, A., Long, G. R., and Piskorski, P. (**1998**). "Modeling otoacoustic emission and hearing threshold fine structures," J. Acoust. Soc. Am. **104**, 1517–1543.
Talmadge, C. L., Tubis, A., Long, G. R., and Tong, C. (**2000**). "Modeling the combined effects of basilar membrane nonlinearity and roughness on stimulus frequency otoacoustic emission fine structure," J. Acoust. Soc. Am. **108**, 2911–2932.
van Dijk, P., and Manley, G. A. (**2001**). "Distortion product otoacoustic emissions in the tree frog Hyla cinerea," Hear. Res. **153**, 14–22.
von Bekesy, G. (**1960**). *Experiments in Hearing* (McGraw Hill, New York).
Wilson, J. P. (**1980**). "Model for cochlear echoes and tinnitus based on an observed electrical correlate," Hear. Res. **2**, 527–532.
Yoon, Y. J., Puria, S., and Steele, C. R. (**2006**). "Intracochlear pressure and organ of corti impedance from a linear active three-dimensional model, Journal for Oto-Rhino-Laryngology and Related Specialities **68**, 365–372.
Zweig, G., and Shera, C. A. (**1995**). "The origin of periodicity in the spectrum of evoked otoacoustic emissions," J. Acoust. Soc. Am. **98**, 2018–2047.